

EN STRONG INTERACTIONS

by



JOHN A. JOHNSTONE, B.Sc.

A Thesis

Submitted to the Faculty of Graduate Studies

in Partial Fulfilment of the Requirements

for the Degree

Master of Science

McMaster University

August 1979

EN STRONG INTERACTIONS

MASTER OF SCIENCE (1979)  
(Physics)

MCMMASTER UNIVERSITY  
Hamilton, Ontario

TITLE: EN Strong Interactions

AUTHOR: John A. Johnstone, B.Sc.

SUPERVISORS: Dr. R. K. Bhaduri, Dr. J. Law (Guelph)

NUMBER OF PAGES: vi, 83

## ABSTRACT

The available  $\Sigma^-$  atomic and  $\Sigma^-N$  scattering data are fitted consistently within a finite range potential model.

The most recent analysis of  $\Sigma^-N$  scattering data produced two possible sets of complex scattering lengths consistent with the observed cross-sections. These data, together with the measured energy level shifts and widths in  $\Sigma^-$  atoms, are analyzed to determine if the combined data are consistent and also to extract effective  $\Sigma^-N$  potentials.

The calculations are performed by assuming Yukawa-shaped complex potentials for each  $\Sigma^-N$  spin, isospin channel. These potentials are then folded into the nuclear density distribution to produce the  $\Sigma^-$ -nucleus effective potential and the Schrödinger equation solved for the level widths and shifts. The potential depths and range are treated as parameters which are varied to minimize the total  $\chi^2$  of the fit to the scattering lengths and atomic data. The possibilities of attractive or repulsive potentials are examined for those  $\Sigma^-N$  channels which produce positive scattering lengths.

Although the results of this analysis indicate that the atomic data can be fitted consistently with the scattering data, there is no conclusive distinction between the two sets of scattering lengths in this respect.

It is concluded however that the existence of a  $\Sigma^- n$  bound state is unlikely and that the  $\Sigma^- n$  spin triplet potential at least must be repulsive.

## ACKNOWLEDGEMENTS

From among the many colleagues and friends whose help and guidance were so valuable to me in the development of this work, I should like in particular to record my indebtedness to Dr. J. Law for suggesting the concept of this thesis; to Dr. A. Deloff for the benefit of his interest and constructive comments; to Dr. R. K. Bhaduri for his continuous support and encouragement, and to Helen Kennelly for producing the final typewritten text with such meticulous care.

To all these members of the university community, I gladly accord my thanks and appreciation.

## TABLE OF CONTENTS

	<u>PAGE</u>
CHAPTER 1 INTRODUCTION	1
CHAPTER 2 $\Sigma$ N SCATTERING	
2.1 Introduction	7
2.2 $\Sigma^-$ p Two-Channel Effective Potential	9
2.3 $\Sigma^-$ N Scattering Cross-Section	13
2.4 Scattering Results	18
CHAPTER 3 $\Sigma$ ATOMS	
3.1 Introduction and Phenomenological Survey of Hadronic Atoms	21
3.2 $\Sigma^-$ Nucleus Folding Model Potential	28
3.3 Spin-Dependent $\Sigma^-$ N Potentials in the Folding Model	35
3.4 Complex Level Shifts Determined from the Schrodinger Equation	39
CHAPTER 4 $\Sigma$ N POTENTIAL OPTIMIZATION	
4.1 Scattering Length Calculations	43
4.2 $\Sigma$ Atom Complex Shift Calculations	49
4.3 Potential Optimization Calculations	53
4.4 $\Sigma$ Hypernuclei	58
CHAPTER 5 CONCLUSIONS	61
APPENDIX A ITERATIVE SOLUTION TO POTENTIAL FOR KNOWN SCATTERING LENGTHS	63
APPENDIX B $\Sigma$ ATOM COMPLEX ENERGY SHIFTS	66
APPENDIX C POTENTIAL OPTIMIZATION PROGRAM	70
REFERENCES	82

CHAPTER 1  
INTRODUCTION

The aim of this work initially was to determine the general nature of the  $\Sigma N$  potentials and, specifically, to determine if a  $\Sigma^- n$  or  $\Sigma^- nn$  bound state is likely. As will be seen, the available  $\Sigma N$  experimental data required this aim to be modified somewhat.

The motivation for the study was the fact that to date, of the baryons, only the proton and neutron are known to form a stable bound state. The  $\Sigma^-$  hyperon is not stable in interacting with a proton and the system decays via the strong interaction to a  $\Lambda$  and neutron, but the  $\Sigma^- n$  system has no corresponding decay channel consistent with charge and energy conservation. It is possible therefore that  $\Sigma^- n$  or  $\Sigma^- nn$  could form a bound state, although to date they have never been observed.

The information available on the  $\Sigma N$  interactions is very scarce, due mainly to the short  $\Sigma$  lifetime, and until 1978 the only information came from  $\Sigma^+ p$  scattering experiments.

The data from these experiments provided many interesting but sometimes ambiguous indications of the  $\Sigma N$  potentials. Alexander et al<sup>(3)</sup> have made the most recent correlation of  $\Sigma N$  scattering parameters. Most notable of their results is the



prediction of a positive scattering length in  $\Sigma^- n \ ^3S_1$  state which could result from a strongly attractive potential with a bound state.

In addition, in  $\Lambda p$  scattering, a cusp in the cross-section below the  $\Sigma$  threshold has been interpreted by some as a virtual  $\Sigma N$  bound state<sup>(26)</sup>. Indeed, in first approximation, a  $\Sigma N$  bound state is to be expected.  $SU(3)$  with no symmetry breaking predicts the  $\Sigma N$  interaction to be identical with the  $NN$  interaction, which is known to be strongly attractive. It might be expected then that the larger  $\Sigma$  mass would lead to a bound state, even though in other respects the scattering data refute this idea.

If the positive  $\Sigma^- n$  scattering lengths of Alexander are the result of a strong, attractive potential, the resulting binding energy of the system would be of the order of 75 Mev. This is huge relative to the deuteron and, although this does not mean it is impossible, the magnitude of  $SU(3)$  symmetry breaking required to produce this binding makes the suggestion highly improbable.

The alternative is that the positive scattering length arises from a repulsive potential. Again, this suggestion is unusual and not generally expected from the strong interaction. However, the OBEP model predicts that in the long-range tail of the potential at least the  $\Sigma^- n \ ^3S_1$  potential should be repulsive.

Furthermore, the total scattering cross-section<sup>(3,22,23,26)</sup> falls below even the singlet unitary limit, which indicates a weak triplet interaction.

The proposal is that a  $\Sigma^-n$  or  $\Sigma^-nn$  bound state exists is not new and has already been investigated to some extent (for example ref. 29). At that time the analyses were based on inaccurate scattering data and even the sign of the scattering lengths was not well known<sup>(30)</sup>. The conclusion of those works was that the  $\Sigma^-n$  interaction was too weak to support a bound state even in the proposed three-body  $\Sigma^-nn$  system.

The difficulty in performing an analysis based solely on scattering data is that a knowledge of the scattering lengths alone does not permit a unique determination of both the depth and range of a two parameter potential form. Even the recent data of Alexander do not determine the effective ranges of the interactions, and in fact produce two distinct sets of scattering lengths consistent with the measured cross-sections.

However, Batty et al<sup>(1)</sup> in 1978 produced  $\Sigma^-$  exotic atoms from stopping  $K^-$  beams. From the strong interaction between the  $\Sigma^-$  and nucleus, the energy of the  $\Sigma^-$  atomic orbital is shifted relative to the pure electromagnetic energy. The energy width of the level is also increased as a result of  $\Sigma^-p$  decay. The magnitude of this complex energy shift is related to the  $\Sigma N$  potentials.

For the first time then, two independent sets of data

4

are now available related to the  $\Sigma N$  interactions. It is possible, by requiring consistency, to analyze the  $\Sigma N$  scattering and  $\Sigma$  atomic data simultaneously and to fix both a potential depth and range to the  $\Sigma N$  interactions. Consequently the purpose of this work now becomes twofold: Not only is an attempt made to extract effective  $\Sigma N$  two-body potentials from a correlation of the data but also to determine if the  $\Sigma$  atomic data are sensitive to the scattering parameters and can distinguish between the two scattering length sets of Alexander.

The basic requirement in realizing this program is the construction of effective  $\Sigma N$  potential forms. In this work it is assumed that the potentials are Yukawa-shaped, with the strengths complex for  $\Sigma^- p$  interactions and real for  $\Sigma^- n$ . The complex  $\Sigma^- p$  depth is introduced to account implicitly for the open decay channel in this system. Atomic level shifts are sensitive, in first approximation, only to the volume integral of the two-body potential and not to the shape<sup>(14)</sup>. In view of this, the Yukawa-shape is chosen to produce the known asymptotic form of the OBE potential tail. A more realistic shape should include a repulsive core; but any refinements of the potential necessarily introduce more parameters and with the present quality and quantity of  $\Sigma N$  data, this would be unwarranted.

The available  $\Sigma N$  scattering data are reviewed in Chapter 2, beginning with the coupled, two-channel formalism of

the  $\Sigma^-p$  scattering process. Decoupling of the  $\Lambda n$  channel results in an effective non-local, complex potential in the  $\Sigma^-p$  channel. Discussion of the non-local, complex potential covers absorption in the  $\Sigma^-p$  system as well as the approximations involved in replacing it with a local, complex potential.


The differential cross-sections for the  $\Sigma^-p$  interactions are also produced showing the relationship between the measured cross-sections and corresponding scattering lengths. The effects of the Coulomb scattering amplitude on the cross-section are included. Although the cross-sections are not explicitly used in this work, the  $\Sigma^-n$  scattering lengths are deduced from the  $\Sigma^+p$  data, and it is therefore necessary to realize the approximations involved in deriving the  $\Sigma^+p$  scattering lengths when the Coulomb interaction is present.

The deriving of an expression for the  $\Sigma^-$ -nucleus effective potential in  $\Sigma$  atoms is dealt with in Chapter 3, commencing with a qualitative survey of hadronic atom properties in general. Attention is drawn to the theoretical approach that has been most commonly used to date and to its shortcomings. A model for the  $\Sigma$ -nucleus potential based on folding the  $\Sigma N$  potentials into the nuclear density is derived. It is shown that, with certain restrictive approximations, the folding model reduces to the common, first-order optical model. Lastly, a prescription is developed for properly weighting the

different spin, isospin  $\Sigma N$  potentials in the folding model.

Numerical details are offered in Chapter 4. A simultaneous fitting procedure is performed to each set of  $\Sigma N$  scattering lengths with the  $\Sigma$  atom complex energy shift data. The  $\Sigma N$  potential strength and range parameters are treated as variables and the total  $\chi^2$  of the fits to all the data is minimized. For those states with positive scattering lengths both strongly attractive and repulsive potential possibilities are considered. In this way six minima are found in the  $\chi^2$  curve. Four of these solution sets are discarded for predicting unphysical binding energies in  $\Sigma N$  systems. The remaining two sets of optimized potentials are used to determine the ground state energies of various proposed  $\Sigma$  hypernuclei.

In conclusion, the results and predictions of the  $\Sigma N$  potentials are summarized and compared with the expected properties from experiment and theory.



Q

CHAPTER 2  
ΣN SCATTERING

2.1: INTRODUCTION

A great deal of interest has been shown in the ΣN scattering process as a means of discovering possible ΣN bound states.

A  $\Sigma^-n$  or  $\Sigma^+p$  bound state has never been found although in SU(3) with no symmetry breaking the singlet  $\Sigma^-n(\Sigma^+p)$  interaction is identical to the NN interaction. The pp and nn potentials are known to be strongly attractive which suggests that the larger Σ mass might be able to produce a bound state<sup>(26)</sup>. In addition, it has been proposed that the resonance in the  $\Lambda p$  scattering cross-section at roughly 4 Mev below the Σ threshold corresponds to a virtual ΣN  $I = \frac{1}{2}$  bound state<sup>(23,26)</sup>.

However, a recent study of the ΣN scattering parameters by Alexander<sup>(3)</sup>, and also the results of the present work, indicate that the existence of a  $\Sigma^-n$  or  $\Sigma^+p$  bound state is unlikely.

The existing data on ΣN scattering are very scarce. This is due, in part, to the short Σ lifetime ( $\sim 10^{-19}$  secs.) and to the fact that the production of Σ is a secondary reaction from stopping  $K^-$  beams so that the number of Σ events

observed is low (typically,  $\sim 10^3$   $\Sigma$  scattering events per  $10^7$   $K^-$  stopped (22)).

The  $\Sigma$  scattering to date has been performed in hydrogen bubble chambers with the result that only  $\Sigma$ -proton events have been measured. The corresponding momentum range of the  $\Sigma$  is roughly  $100 \leq p_\Sigma \leq 180$  Mev/c. The lower limit is imposed experimentally by the length of the  $\Sigma$  tracks and the upper limit is the production momentum of the  $\Sigma$  in the reaction  $K^- + p \rightarrow \Sigma^\pm + \pi^\mp$  (22). The  $\Sigma^-$  is not stable in the presence of protons and decays by the strangeness-conserving reaction:



The  $|\Sigma^- N\rangle$  wavefunction can be expanded in isospin components as:

$$\begin{aligned} |\Sigma^- N\rangle &\equiv |I_\Sigma I_\Sigma I_N I_N\rangle , \\ &= \sum_I \langle I-1 \frac{1}{2} I \frac{1}{2} | I I \rangle |I I\rangle |I I\rangle \end{aligned} \quad (2.1.2)$$

with the weighting given by Clebsch-Gordan coefficients. For  $\Sigma^- p$   $I_3^p = \frac{1}{2}$  and the  $|\Sigma^- p\rangle$  wavefunction becomes:

$$|\Sigma^- p\rangle = \sqrt{\frac{2}{3}} \left| \frac{1}{2} - \frac{1}{2} \right\rangle + \sqrt{\frac{1}{3}} \left| \frac{3}{2} - \frac{1}{2} \right\rangle , \quad (2.1.3)$$

which explains the presence of the  $I = \frac{1}{2}$   $\Lambda$  decay channel in  $\Sigma^- p$  scattering. The  $\Sigma^- n$  ( $\Sigma^+ p$ ) system however is a pure  $I = \frac{3}{2}$  state and can only scatter elastically.

## 2.2: $\Sigma^-p$ TWO-CHANNEL EFFECTIVE POTENTIAL

It is clear from the discussion in the last section that the  $\Sigma^-p$  system can either scatter elastically to the  $\Sigma^-p$  final state or decay through the strong interaction to a  $\Lambda n$  state. A proper description of the scattering process must account for this two-channel nature.

The expansion of the usual one-channel scattering theory to describe the two-channel problem is straightforward with the important result that the wavefunction has two components and the potential becomes a  $2 \times 2$  matrix. The off-diagonal potential elements couple the wavefunction components through the two radial Schrodinger equations:

$$-\frac{\hbar^2}{2M_{\Sigma p}} \psi_{\Sigma}'' + V_{\Sigma\Sigma} \psi_{\Sigma} + V_{\Sigma\Lambda} \psi_{\Lambda} = E_{\Sigma} \psi_{\Sigma} \quad (2.2.1)$$

$$-\frac{\hbar^2}{2M_{\Lambda n}} \psi_{\Lambda}'' + V_{\Lambda\Sigma} \psi_{\Sigma} + V_{\Lambda\Lambda} \psi_{\Lambda} = E_{\Lambda} \psi_{\Lambda} \quad (2.2.2)$$

The energy  $E_{\Lambda}$  appearing in the  $\Lambda n$  equation (2.2.2) is related to the energy of the  $\Sigma^-p$  system by the mass difference of the  $\Sigma^-$  and  $\Lambda$ ; that is:

$$E_{\Lambda} = E_{\Sigma} - \Delta M_{\Sigma\Lambda} \quad (2.2.3)$$

These coupled equations can be solved numerically provided the four potential elements are known.



Formally, the two-channel equations can be decoupled by inverting the  $\Lambda n$  equation. For the  $\Lambda n$  channel:

$$\psi_{\Lambda n} = -V_{\Lambda\Sigma} \frac{1}{\left(-\frac{\hbar^2}{2M_{\Lambda n}} \frac{d^2}{dr^2} + V_{\Lambda\Lambda} - E_{\Lambda} - i\epsilon\right)} \cdot \psi_{\Sigma p} \quad (2.2.4)$$

Substituting this expression into (2.2.1) produces the  $\Sigma^- p$  channel equation:

$$\frac{d^2\psi_{\Sigma}}{dr^2} - \frac{2M_{\Sigma p}}{\hbar^2} (V_{\Sigma\Sigma} - V_{\Sigma\Lambda} \cdot \frac{1}{(T_{\Lambda} + V_{\Lambda\Lambda} - E_{\Lambda} - i\epsilon)} \cdot V_{\Lambda\Sigma}) \psi_{\Sigma} = -k_{\Sigma}^2 \psi_{\Sigma} \quad (2.2.5)$$

or

$$\frac{d^2\psi_{\Sigma}}{dr^2} - \frac{2M_{\Sigma p}}{\hbar^2} \cdot V_{\text{EFF}} \cdot \psi_{\Sigma} = -k_{\Sigma}^2 \psi_{\Sigma} \quad (2.2.6)$$

The important features of the effective  $\Sigma^- p$  potential  $V_{\text{EFF}}$  is that it is non-local and complex. The  $-i\epsilon$  term has been introduced in the denominator to ensure that the open  $\Lambda n$  channel contains only outgoing waves.

The potential  $V_{\text{EFF}}$  may be expanded in the spectral representation as <sup>(25)</sup>:

$$V_{\text{EFF}} = V_{\Sigma\Sigma} - \sum_n V_{\Sigma\Lambda} \frac{|\psi_{\Lambda}^{(n)}\rangle \langle \psi_{\Lambda}^{(n)}|}{E^{(n)} - E} V_{\Lambda\Sigma} - \int_{\Delta M}^{\infty} dE' V_{\Sigma\Lambda} \frac{|\psi_{\Lambda}(E')\rangle \langle \psi_{\Lambda}(E')|}{E' - E - i\epsilon} V_{\Lambda\Sigma} \quad (2.2.7)$$

where the discrete summation corresponds to possible bound states in the  $\Lambda n$  system. Assuming that no such states exist,  $V_{\text{EFF}}$  can be written explicitly in terms of its real and imaginary

components as (21):

$$V_{\text{EFF}} = V_{\Sigma\Sigma} - P \int_{\Delta M}^{\infty} \frac{V_{\Sigma\Lambda} |\psi_{\Lambda}\rangle \langle \psi_{\Lambda}| V_{\Lambda\Sigma}}{E' - E} dE' - i\pi \int dE' \delta(E' - \Delta M) V_{\Sigma\Lambda} |\psi_{\Lambda}\rangle \langle \psi_{\Lambda}| V_{\Lambda\Sigma} \quad (2.2.8)$$

where P denotes the Cauchy principal value. The imaginary part of the potential is then:

$$\begin{aligned} \text{Im}(V_{\text{EFF}}) &= -\pi \cdot V_{\Sigma\Lambda} |\psi_{\Lambda}\rangle \langle \psi_{\Lambda}| V_{\Lambda\Sigma} \quad , \quad E = \Delta M \quad , \\ &= 0 \quad , \quad E < \Delta M \quad . \end{aligned} \quad (2.2.9)$$

Since the numerator of the real part of  $V_{\text{EFF}}$  is positive definite, the imaginary component is negative definite as required for absorption. Physically the complex term comes from the process in which the  $\Sigma^-$  and p leave the entrance channel  $\psi_{\Sigma}$  because of the coupling potential  $V_{\Lambda\Sigma}$  and are emitted in the exit channel  $\psi_{\Lambda}$ .

To see how the complex potential accounts for absorption in  $\Sigma^-p$  scattering, it can be shown from the Schrodinger equation that the divergence of the flux for a complex potential is:

$$\nabla \cdot \underline{j}(\underline{r}, t) = \frac{2}{\hbar} \text{Im}(V) \rho(\underline{r}) \quad , \quad (2.2.10)$$

with  $\rho(\underline{r})$  the probability density. It has been shown that the imaginary component of  $V_{\text{EFF}}$  is negative which, according to (2.2.10), accounts for a loss of particles from the system.

Further, the time development of the  $\Sigma^-$  p wavefunction is:

$$\psi_{\Sigma}(t) \propto e^{-iEt/\hbar} \quad (2.2.11)$$

For a complex potential the energy of the system  $E_{\Sigma}$  is necessarily also complex. With the definition  $E_{\Sigma} \equiv E_R + i\Gamma/2$ , the time development of the wavefunction becomes:

$$\psi_{\Sigma}(t) \propto e^{-E_R t/\hbar} e^{-\Gamma t/2\hbar}, \quad (2.2.12)$$

which is a damped function corresponding to a decrease in the number of  $\Sigma^-$  as a function of time.

In solving the  $\Sigma^-$  p radial equation (2.2.6) it has been shown possible to replace  $V_{\text{EFF}}$  with a phase-equivalent local potential which correctly reproduces the two-channel scattering lengths<sup>(24)</sup>. However, the expression for the potential is a complicated function of the matrix elements  $V_{YY}$  and both wavefunction components. Without a firm theoretical basis for determining the  $V_{YY}$  though, there does not appear to be any clear advantage to this procedure. As a first approximation, the usual approach (and the one used in this work) is to ignore the non-local and energy-dependent behaviour of  $V_{\text{EFF}}$  and approximate  $V_{\text{EFF}}$  with a complex, local potential. In this way the two-channel nature of the problem is implicitly introduced through the complex potential depth.

The theory of scattering for a local, complex potential is essentially the same as for real potentials with the

important exception that the phase shifts and scattering lengths become complex corresponding to a decrease in amplitude of the wavefunction<sup>(25)</sup>.

### 2.3: $\Sigma^- N$ SCATTERING CROSS-SECTION

The spatial distribution of reaction products from a scattering process is dependent on the nature of the interaction between the projectile and target. At low incident energies the most that can be learned about the potential though, is the corresponding scattering lengths or phase shifts.

In deriving expressions for the  $\Sigma^- p$  cross-sections as functions of the scattering lengths it will be assumed at first that the Coulomb interaction can be neglected. This is an important correction, particularly for small scattering angles, and will be included later, but it is not necessary for outlining the approach. The notation used follows closely that of references 3 and 23. It is also assumed that the interaction occurs only in S-state and that the singlet and triplet interactions can be treated separately.

The cross section for a transition from an initial state  $|\Sigma^- p\rangle$  to a final state  $|f\rangle$  is related to the transition matrix by<sup>(23)</sup>:

$$\sigma(\Sigma^- p \rightarrow f) = \frac{4\pi^2 (2J+1)}{k(2S_{\Sigma}+1)(2S_p+1)} |\langle \Sigma p | T | f \rangle|^2, \quad (2.3.1)$$

with  $k$  the centre of mass momentum and  $J$  the total angular

momentum of the  $\Sigma^- p$ .  $S_\Sigma$  and  $S_p$  are the spins of  $\Sigma^-$  and  $p$  respectively.

From the two-channel nature of this problem, the  $T$  matrix has four components;  $T_{\Sigma\Sigma} = \langle \Sigma p | T | \Sigma p \rangle$ ,  $T_{\Sigma\Lambda} = \langle \Sigma p | T | \Lambda n \rangle$ , et. cetera.

For the elastic scattering of  $\Sigma^- p \rightarrow \Sigma^- p$  the transition amplitudes can be expressed as functions of the complex scattering lengths at low energy by:

$$\langle \Sigma p | T | \Sigma p \rangle = \frac{A}{1 - ikA}, \quad (2.3.2)$$

with  $A = a + ib$ , the complex scattering length. In the  $\Sigma^- p$  interaction  $\frac{2}{3}$  of the transitions occur in the  $I = \frac{1}{2}$  state and  $\frac{1}{3}$  in the  $I = \frac{3}{2}$  state. Using this fact, straightforward algebra gives the  $\Sigma^- p$  elastic cross-section as:

$$\sigma(\Sigma^- p \rightarrow \Sigma^- p) = \frac{\pi}{9} \sum_{J=0}^{\infty} (2J+1) \left( (a_{J3/2} + 2a_{J1/2} + 3ka_{J3/2}b_{J1/2})^2 + (2b_{J1/2} - 3ka_{J3/2}a_{J1/2})^2 \right) / (1+k^2a_{J3/2}^2)(1+k^2(a_{J1/2}^2 + b_{J1/2}^2)), \quad (2.3.3)$$

where  $A_{JI} = a_{JI} + ib_{JI}$  is the complex scattering length in the  $J, I$  spin, isospin channel. Use has also been made of the fact that  $b_{J3/2} = 0$  since there can be no inelastic scattering in the  $\Sigma^- n$  interaction.

For the inelastic  $\Sigma^- p \rightarrow \Lambda n$  channel a simple expression like (2.3.2) does not exist and more care must be exercised

in defining the T matrix. It can be shown from a K-matrix analysis of the scattering lengths<sup>(23)</sup> that the transition amplitude for the inelastic process can be expressed as:

$$\langle \Sigma p | T | \Lambda n \rangle = \frac{1}{1 - ikA} \frac{\langle \Sigma p | K | \Lambda n \rangle}{1 - i \langle \Lambda n | K | \Lambda n \rangle}, \quad (2.3.4)$$

where A in this case is the  $I = \frac{1}{2}$  scattering length  $a_{J1/2} + ib_{J1/2}$  for the decay channel. Rewriting A in terms of the K matrix, Gell et al also show that:

$$\begin{aligned} \left| \frac{\langle \Sigma p | K | \Lambda n \rangle}{1 - i \langle \Lambda n | K | \Lambda n \rangle} \right|^2 &= \left| \frac{A - \langle \Sigma p | K | \Sigma p \rangle}{1 - i \langle \Lambda n | K | \Lambda n \rangle} \right|^2 \\ &= kb_{J1/2}^2, \end{aligned} \quad (2.3.5)$$

where the last step follows from the relation of the K matrix to the scattering lengths.

The cross-section for the inelastic  $\Sigma^- p$  reaction is then:

$$\sigma(\Sigma p \rightarrow \Lambda n) = \frac{2\pi}{3k} \sum_{J=0}^{\infty} (2J+1) \frac{b_{J1/2}^2}{1 + k^2 (a_{J1/2}^2 + b_{J1/2}^2)}. \quad (2.3.6)$$

The above expressions (2.3.3) and (2.3.6) were evaluated neglecting the Coulomb interaction between the  $\Sigma^-$  and p. Since the Coulomb potential goes to zero only as quickly as  $\frac{1}{r}$  it is to be expected that its presence will have a significant effect on the scattering cross-sections. The procedure for handling

the Coulomb potential when other forces are present is to split the Hamiltonian into a Coulomb and a nuclear part. The T matrix may then be expressed as a sum of a pure Coulomb T matrix and a T-like matrix of the nuclear interaction. The expression for this latter T though does not contain the usual plane-wave state, but rather the Coulomb wavefunction.

If the nuclear potential is spherically symmetric, the amplitude can be expanded in partial waves:

$$A^{NC}(\underline{k}', \underline{k}) = 4\pi \sum_{\ell} Y_{\ell}^{m*}(\hat{k}) a_{\ell}(k) Y_{\ell}^m(\hat{k}') . \quad (2.3.7)$$

The pure Coulomb amplitude is well known (see, for example ref. 26) and is:

$$A^C(\theta) = \frac{\exp((2i/kB) \ln \sin \theta/2)}{2k^{-1} B \sin^2 \theta/2} , \quad (2.3.8)$$

With B the Bohr radius of the particles, k the centre-of-mass momentum and  $\theta$  the scattering angle.

The cross-section will now contain an interference term between  $A^{NC}$  and  $A^C$  upon squaring their sum. Since the phase of  $A^C$  depends strongly on the charges of the particles, so does the interference term.

Of greatest consequence in the calculation of  $A^{NC}$  is that the usual free wavefunctions become Coulomb wavefunctions. The implication of this is that the additional phase shift introduced in the wavefunction by the nuclear interaction in

the presence of a Coulomb potential is not the same as the effect of the nuclear interaction alone. The result is that there is no longer a simple relationship between  $A^{NC}$  and the nuclear scattering lengths.

Only within certain approximations of the Coulomb wavefunctions dependent on the range of the nucleus interaction can the amplitude  $A^{NC}$  be related to the nuclear scattering lengths. Including the Coulomb amplitude within the differential cross-section and evaluating the nuclear amplitude with respect to approximate Coulomb waves, Alexander et al arrive at the following expressions for the  $\Sigma^-p$  cross-sections <sup>(3)</sup>:

$$\frac{d\sigma}{d\Omega} (\Sigma^-p \rightarrow \Sigma^-p) = \sum_{J=0} \frac{1}{4} (2J+1) \left| \frac{\exp((2i/kB) \ln \sin \theta/2)}{2k^2 B \sin^2 \theta/2} + \frac{C_0^2 (A_{J3/2} + 2A_{J1/2} - 3ikA_{J1/2}A_{J3/2})}{D_J} \right|^2 \quad (2.3.9)$$

$$\frac{d\sigma}{d\Omega} (\Sigma^-p \rightarrow \Lambda n) = \frac{1}{k} \sum_{J=0} (2J+1) \left| \frac{C_0 (1 - ikA_{J3/2})}{D_J} \right|^2 b_{J1/2} \quad (2.3.10)$$

with

$$D_J = 3 - ik(A_{J1/2} + 2A_{J3/2}) - kC_0^2 (1 - i\lambda) (i(A_{J3/2} + 2A_{J1/2}) + 3kA_{J1/2}A_{J3/2})$$

$$C_0 = \frac{2\pi}{kB} (1 - \exp(-\frac{2\pi}{kB}))^{-1}$$

and

$$\lambda = - \frac{2(\ln(2kR) + \text{Re}\Psi(i/kB) + 2\gamma)}{kBC_0^2}$$



## 2.4: SCATTERING RESULTS

The experimental scattering situation has changed drastically in the last few years as more data are collected and the accepted scattering lengths for the  $\Sigma N$  system have changed by as much as 100 per cent. To a large extent this is because earlier works (22,23,26) neglected the important Coulomb contribution to the cross-section.

The data have presented some interesting features and raised many questions.

The total elastic  $\Sigma^{\pm} p$  cross-sections are shown in figure 2.1 with the solid line representing the spin singlet unitary limit.

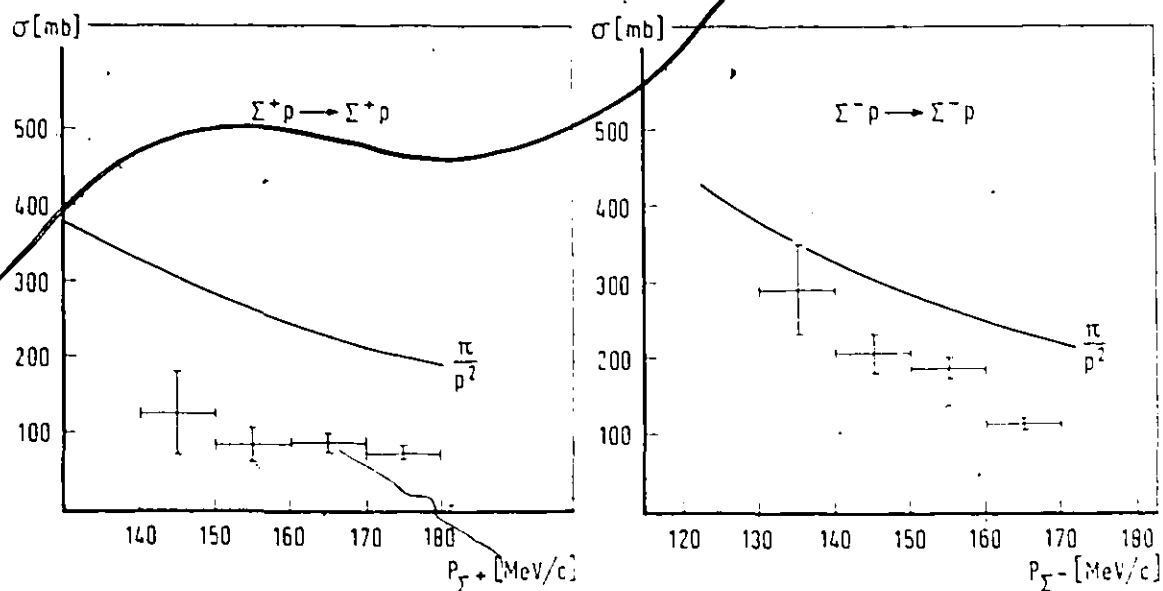


FIG. 2.1 ELASTIC  $\Sigma^{\pm} p$  CROSS SECTIONS (REF. 26 AND REFERENCES THEREIN).

The total cross-sections are lower than the singlet unitary limit, which has been taken as an indication that the triplet interaction must be very weak and a bound state in the  $^3S_1$  interaction therefore unlikely.

The elastic  $\Sigma^-p$  differential cross-section  $\sigma(\theta)$  is shown in figure 2.2. The apparent systematic rise in  $\sigma(\theta)$  for small angles can be attributed to constructive Coulomb interference <sup>(3)</sup>.

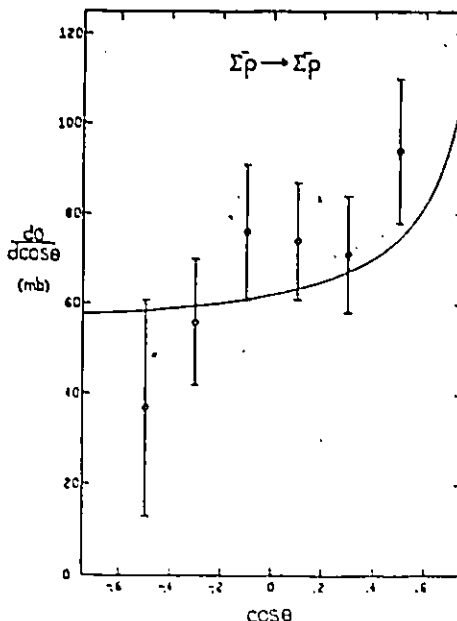


FIG. 22  $\Sigma^-p$  ELASTIC DIFFERENTIAL CROSS-SECTION. DATA POINTS ARE FROM ALEXANDER (3). SOLID LINE IS  $\sigma(\theta)$  PREDICTED FROM THE RESULTS OF THE PRESENT WORK (CHAPT. 4).

The total inelastic  $\Sigma^-p$  cross-section is shown in figure 2.3 and it is found to correspond well with the singlet unitary limit, again indicating a small amplitude in the  $^3S_1$  state.

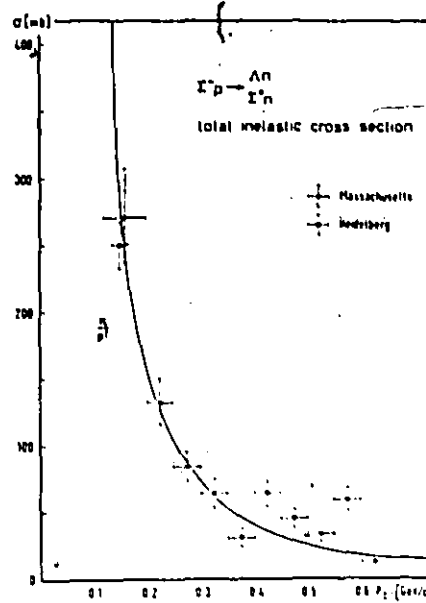


FIG. 2.3 INELASTIC  $\Sigma^- p$  CROSS-SECTION  
(REF. 26).

The most recent data on  $\Sigma^\pm p$  scattering have been collected by Alexander et al<sup>(3)</sup>. They constructed scattering lengths in the complex plane for each spin, isospin channel which would reproduce the observed total cross-sections. By treating the components of the complex scattering lengths as parameters they fitted the data and found two sets of scattering lengths consistent with the cross-sections. Because of the large errors in the cross-section data they could not distinguish between these sets, but neither set supported the suggestion of an  $I = \frac{1}{2}$  virtual  $\Sigma N$  bound state.

The results of the present work also point to the same conclusion. In this work the  $\Sigma^- n$  scattering lengths are presumed identical to the  $\Sigma^+ p$  extracted nuclear scattering

lengths, based on the assumptions of charge and isospin invariance of the interactions.

One of the purposes of the present work is to correlate Alexander's scattering lengths with  $\Sigma$  atom data in an attempt to distinguish between the two sets he obtained.

Contrary to the results of a previous analysis<sup>(1)</sup>, it is found that the atomic data are consistent with the scattering lengths but, because of the large experimental errors, the atomic data do not distinguish between the two sets.

## CHAPTER 3

### $\Sigma$ ATOMS

#### 3.1: INTRODUCTION AND PHENOMENOLOGICAL SURVEY OF HADRONIC ATOMS

Hadronic atoms are those in which an electron has been replaced by a strongly-interacting particle ( $K^-$ ,  $\pi^-$ ,  $\bar{p}$ ,  $\Sigma^-$ ).

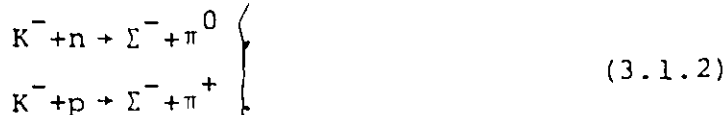
Creating hadronic atoms is experimentally relatively simple although the high energies involved restrict their formation to only a few laboratories in the world.

Kaons are produced primarily by the reactions:



The primary target for the reactions (3.1.1) is normally a heavy metal. The  $K^-$  produced travel to a secondary target where they are slowed and eventually captured into atomic orbitals.

The picture is not as simple for  $\Sigma^-$  atoms.  $\Sigma^-$  hyperons are created from the nuclear absorption of  $K^-$  mesons through the reactions:



Because the  $\Sigma^-$  are produced in secondary reactions, the resulting  $\Sigma^-$  atom x-ray spectra are very low intensity and necessarily buried in the predominant  $K^-$  atomic spectra.

Neglecting the strong interaction, the mean radius of the hadron's atomic orbital about a point nucleus is:

$$\langle r \rangle = \frac{a_0}{2Z} (3n^2 - \ell(\ell+1)) , \quad (3.1.3)$$

where  $a_0$  is the Bohr radius  $= \hbar^2 / e^2 m_H$ ,  $m_H$  is the reduced mass of the hadron-nucleus system, and  $n, \ell$  are the orbital quantum numbers. In a first approximation then, the  $\Sigma^-$  orbital radius is reduced by a factor of nearly 2400 relative to the corresponding electron orbital with the result that even in high  $n$  states the  $\Sigma^-$  is closer to the nucleus than the ground state electrons. Electronic screening of the nucleus by the electrons therefore has a negligible effect and the hadron-nucleus system can be accurately treated as a true two-body interaction.

In addition to the electromagnetic interaction the orbiting hadron is affected by the strong force. This nuclear force manifests itself predominantly in two ways. The energy of the orbital is shifted relative to the pure electronic energy of the orbital by an amount  $\epsilon$ , and secondly, the absorptive nature of the strong interaction causes a broadening of the natural Lorentzian linewidth by an amount  $\Gamma$ .

Initial capture of the hadron by the atom occurs primarily by Auger emission of an electron leaving the resul-

tant hadronic atom in a state of high excitation and angular momentum. The hadron de-excites by x-ray transitions until a level is reached where there is an appreciable overlap of the hadron wavefunction with the nucleus, and at this point it is absorbed.

In the x-ray transition between the levels  $(n+1, \ell+1) \rightarrow (n, \ell)$ , the width  $\Gamma$  of the upper level is typically of the order of 1 ev. which is comparable to the electronic width. Absorption and x-ray transition processes therefore compete and the branching ratios of the two processes can be measured. Since the strong interaction is short-ranged,  $\epsilon$  for the upper level is essentially zero. The width of the lower level is larger than the upper by a factor of  $10^2-10^3$  due to the greater nuclear overlap. The shift  $\epsilon$  is the same order of magnitude as the lower level width  $\Gamma$ . Measurement of the x-ray energy of the transition then provides a direct measurement of  $\epsilon$ . The strong absorptive interaction sets a lower limit on the angular momentum state in which the hadron can exist. For small values of  $r$ , the Coulomb wavefunctions are proportional to  $\frac{r^\ell}{n}$  which indicates that states of high angular momentum have a smaller overlap with the nuclear volume than those of low  $n$  and  $\ell$ .

In hadronic atoms therefore the transitions of interest are those between the 'circular' orbits, that is, those for which  $\ell = n-1$ . For circular orbits the probability of finding the hadron between  $r$  and  $r+dr$  from the nuclear centre is approximately<sup>(8)</sup>:

$$r^2 \cdot \psi^*(r) \psi(r) dr \sim \frac{1}{(2\ell+1)!} \left(\frac{2Z}{na_0}\right)^{2\ell+3} \frac{r^{2\ell+2}}{2n} e^{-2Zr/a_0 n} dr. \quad (3.1.4)$$

The overlap of the hadron wavefunction with the absorptive part of the hadron-nucleus potential gives an estimate of the region in which absorption occurs. For high  $\ell$  states this is peaked in the area of the nuclear surface as shown in figure 3.1 below.

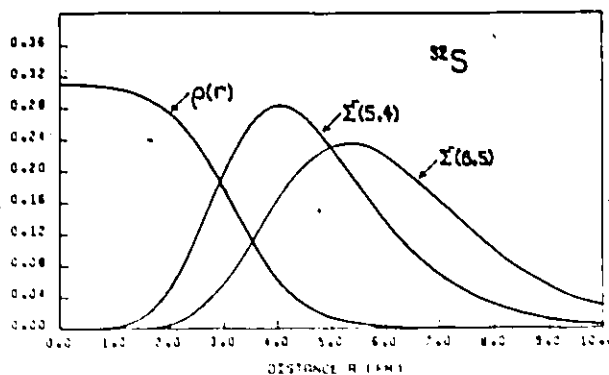


FIG. 3.1 ABSORPTION OF  $\Sigma^-$  FROM  $(n, \ell)$  STATES IN  $^{32}\text{S}$ . CURVES ARE CALCULATED USING RESULTS OF THIS WORK, CHAPTER 4. ALL CURVES NORMALIZED TO UNIT AREA.

It has been stressed<sup>(6,7,9)</sup> that this feature makes hadron absorption a potentially powerful tool for studying the nuclear surface, and in particular for testing the proposal of a neutron-rich surface through a comparison of absorption rates in isotopes. Although some attempts have been made along these lines<sup>(5)</sup>, the data are not yet exact enough to give conclusive results.

Apart from this, hadronic atoms are capable of providing information about the hadrons themselves. Precise measure-



ments of the transition energies give data on some particle properties not accurately known from other sources. Most notable of these are the particle mass and magnetic moment.

The Coulomb energy of a particle interacting with a point-charge nucleus is directly proportional to the reduced mass of the system. The high  $n$  transitions chosen for mass determination are dominated almost exclusively by this energy. The accuracy of determining the mass is then the same as the accuracy of measuring the x-ray transition energy.

In fact, the  $K^-$  mass determined in this way is more accurate than by any other method<sup>(10)</sup>. The same cannot be said for the  $\Sigma^-$  because of the low intensity of x-ray data.

The interest in  $\Sigma^-$  atoms arose as a means of determining the  $\Sigma^-$  magnetic moment<sup>(5)</sup>. The fine-structure splitting between the  $j = \ell + \frac{1}{2}$  and  $\ell - \frac{1}{2}$  states in this case is:

$$\Delta E = \frac{1}{2}(1+g)m_{\Sigma}c^2 \cdot \left(\frac{\alpha Z}{n}\right)^4 \frac{n}{\ell(\ell+1)} \quad (3.1.5)$$

where  $g$  is the anomalous part of the magnetic moment  $\mu = eh(1+g)/2m_{\Sigma}c$ . Measurement of this splitting is particularly difficult for  $\Sigma^-$  atoms. The  $\Sigma^-$  x-ray lines are present only in  $K^-$  spectra whose intensities are an order of magnitude or more larger (see figure 3.2).

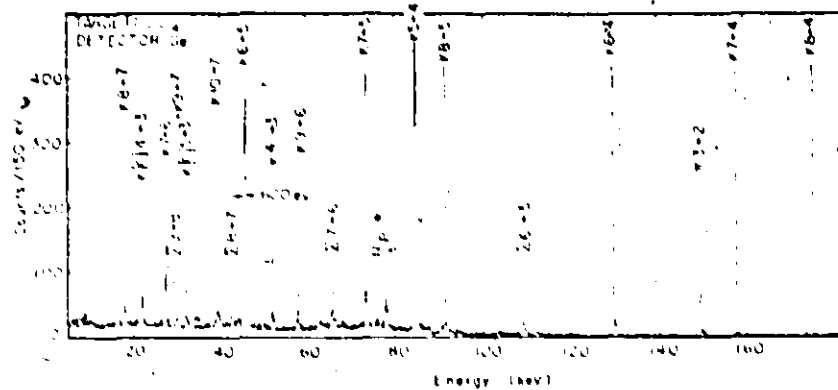


FIG. 3.2  $\Sigma^-$  AND  $K^-$  X-RAY SPECTRA. FROM REF. (5).

The  $\Sigma^-$  magnetic moment determined by this method gives only crude agreement with the predictions of the quark model and SU(3) (11).

The discrepancies are considered an indication of the lack of a firm theoretical basis describing the atomic capture and cascade of the hadrons.

Extraction of the fine structure splitting is strongly dependent on the results of cascade calculations. These calculations have been performed by assuming an initial population distribution with variable parameters and treating the cascade process semi-classically as a continuous energy loss. This dubious procedure has produced only rough agreement with experimental  $K^-$  x-ray intensities (13).

In addition to this area of uncertainty the multi-channel nature of the hadron-N interactions has caused difficulties in constructing a theoretically sound hadron-nucleus

potential. The simplest phenomenological model assumes that the hadron-nucleus potential follows the same shape as the nuclear density with a complex depth adjusted to produce the observed complex energy level shift. Although this procedure gives qualitative agreement with experiment<sup>(1,7,16)</sup> there is no strong justification for the assumed shape.

The main task in the study of hadronic atoms is then constructing a reliable hadron-nucleus potential.

This problem is addressed in the following two sections where a general  $\Sigma^-$  nucleus folding model is developed and compared with more common phenomenological potentials.

### 3.2: $\Sigma^-$ -NUCLEUS FOLDING MODEL POTENTIAL

The most commonly used hadron-nucleus effective potential is the optical model in which the potential depth is linearly related to the hadron-N scattering length  $a$ . In this model the  $\Sigma^-$ N interaction is assumed point-like and given by a potential of the form:

$$v(\Sigma^-N) = 4\pi \cdot \frac{\hbar^2}{2M_{\Sigma N}} \cdot \bar{a} \cdot \delta^3(\underline{r}_N - \underline{r}_\Sigma), \quad (3.2.1)$$

where  $M_{\Sigma N}$  is the reduced mass and  $\bar{a}$  is the average, free  $\Sigma^-$ N scattering length (nuclear physics convention). In the coherent nucleus approximation the  $\Sigma^-$ -nucleus potential is obtained by averaging over the ground state nuclear wavefunction:

$$V_{\Sigma} = \frac{A}{\sum_{i=1}^A} \langle 0 | v_i | 0 \rangle . \quad (3.2.2)$$

The optical potential then takes the form:

$$\frac{2mV_{\Sigma}}{\hbar^2} \sim 4\pi \left(1 + \frac{M_{\Sigma}}{M_N}\right) (Z\bar{a}_{\Sigma p} \cdot \rho_p(r) + N\bar{a}_{\Sigma n} \cdot \rho_n(r)) , \quad (3.2.3)$$

where  $\rho_p(r)$  and  $\rho_n(r)$  are the proton and neutron densities respectively, normalized to unity.  $A$  has been assumed large so that  $M/M_{\Sigma N} \sim 1 + M_{\Sigma}/M_N$ , with  $M$ ,  $M_{\Sigma N}$ ,  $M_{\Sigma}$  and  $M_N$  the  $\Sigma^-$  nucleus reduced mass,  $\Sigma N$  reduced mass,  $\Sigma$  mass and nucleon mass, respectively.

The potential is also applied in the form<sup>(1,7)</sup>:

$$\frac{2m}{\hbar^2} \cdot V_{\Sigma} \sim 4\pi \left(1 + \frac{M_{\Sigma}}{M_N}\right) A\bar{a}\rho(r) , \quad (3.2.4)$$

where it has been assumed that the nucleon densities are the same and  $\bar{a} = (Z\bar{a}_{\Sigma p} + N\bar{a}_{\Sigma n})/A$ . In this model the complex scattering length  $\bar{a}$  simulates the absorptive nature of the  $\Sigma^-$  nucleus interaction.

Although the potential form (3.2.4) produces qualitative agreement with experimentally measured complex energy shifts, it is found that the complex depth  $\bar{a}$  which best fits the shifts bears little resemblance to free scattering length value of  $\bar{a}$ . Koch<sup>(18)</sup>, and Batty<sup>(1)</sup> applied such potential forms to  $K^-$  and  $\Sigma^-$  atoms respectively. Their best fitting values of the parameters  $\bar{a}$  had approximately the same imaginary

part as the free value but grossly different real components. In both cases the authors attribute the discrepancy to the existence of resonances in the interaction. In fact the need to invoke resonances is superficial and will be seen to vanish when the unjustified linear relationship between  $V_{\Sigma}$  and  $\bar{a}$  is removed. This requires a more careful averaging of the many-body wavefunction<sup>(14)</sup>.

Of fundamental importance in this procedure is the coherent nucleus approximation. That is, it is assumed that there is no transfer of kinetic energy from the hadron to the nucleus, or equivalently, that the nucleus remain in the ground state at all times during the interaction. The justification for this approach is that the interaction occurs at low energies, relative to the low-lying nuclear level spacing. With the coherent nucleus approximation it is possible to average over the nuclear degrees of freedom and thereby reduce an  $A+1$  body equation to an effective two body problem.

In averaging the many-body equation the nuclear ground state wavefunction is first expanded in terms of a complete set of nuclear eigenstates:

$$\psi(r_1, r_2, \dots, r_A; r_{\Sigma}) = \sum_i \phi_{Ni}(r_1, r_2, \dots, r_A) \cdot \phi_{\Sigma i}(k, r_{\Sigma}), \quad (3.2.5)$$

where the  $r_i$  are nucleon co-ordinates and  $r_{\Sigma}$  the co-ordinate of the  $\Sigma^-$ . This expression is inserted into the Schrödinger

equation. Premultiplying by  $\phi_{Nj}$  and using the orthonormality of the states  $\phi_N$  leads to:

$$\begin{aligned}
 -\frac{\hbar^2}{2m} \nabla^2 \phi_{\Sigma j}(k, r_{\Sigma}) + \sum_i \langle \phi_{Nj} | v_i(r_{\Sigma} - r_i) | \phi_{Ni} \rangle \cdot \phi_{\Sigma i}(k, r_{\Sigma}) \\
 = \frac{\hbar^2}{2m} k^2 \cdot \phi_{\Sigma j}(k, r_{\Sigma}) , \quad (3.2.6)
 \end{aligned}$$

where  $v_i(r_{\Sigma} - r_i)$  is the two body interaction between the  $\Sigma^-$  and  $i^{\text{th}}$  nucleon.

Equation (3.2.6) represents an infinite number of coupled equations. In the coherent nucleus approximation the potential  $v_i$  cannot couple the nuclear states  $\phi_i$  and  $\phi_j$  for  $i \neq j$  so that the system reduces to a two-body equation with an effective  $\Sigma^-$ -nucleus potential given by:

$$V_{\Sigma}(r) = \langle 0 | \sum_{i=1}^A v_i(r_{\Sigma} - r_i) | 0 \rangle , \quad (3.2.7)$$

and  $|0\rangle$  denotes the nuclear ground state. This expansion cannot be simplified further without adopting a model for the potential shape. For simplicity only a central potential will be considered. In addition, for illustrative purposes it will be assumed that the  $\Sigma^-$ -nucleon interaction is equal in each spin state and for both types of nucleons. In the next section the effective potential will be extended to include the physical situation in which the  $\Sigma^-N$  interactions are unequal.

The two-body potential is considered to be of the form:

$$v(\underline{r}) = v_0 \cdot f(\underline{r}) , \quad (3.28)$$

where  $f(\underline{r})$  is a smooth function of  $\underline{r}$  and  $v_0$  is the complex volume integral. The value of  $v_0$  is such that  $f(\underline{r})$  is normalized to unit volume:

$$\int d\underline{r} f(\underline{r}) = 1 . \quad (3.2.9)$$

The effective potential (3.2.7), then becomes:

$$\begin{aligned} V_{\Sigma} &= \langle 0 | \sum_{i=1}^A v(\underline{r}_{\Sigma} - \underline{r}_i) | 0 \rangle = \langle 0 | \int d\underline{r} \sum_{i=1}^A \delta(\underline{r} - \underline{r}_i) v(\underline{r}_{\Sigma} - \underline{r}) | 0 \rangle , \\ &= \int d\underline{r} v(\underline{r}_{\Sigma} - \underline{r}) \langle 0 | \sum_{i=1}^A \delta(\underline{r} - \underline{r}_i) | 0 \rangle , \end{aligned} \quad (3.2.10)$$

$$= A \cdot \int d\underline{r} v(\underline{r}_{\Sigma} - \underline{r}) \rho(\underline{r}) , \quad (3.2.10)$$

where  $\rho(\underline{r})$  is the nucleon density normalized to one. As a first approximation then the  $\Sigma^-$  nucleus effective potential is just the two-body interaction folded into the nuclear density. The folding model expression may be related to the optical model by the following observations.

It has been shown<sup>(17)</sup> that for simple-shaped potentials the depth can be approximately related to the S-state scattering length by:

$$V_0 \sim 4\pi \frac{\hbar^2}{2M_{\Sigma N}} \frac{\bar{a}}{1 + \bar{a}\mu/Q}, \quad (3.2.11)$$

where  $\mu$  is the inverse range of the potential and  $Q$  is a constant dependent on the shape, but roughly  $\mu/Q \approx 1$ .

The effective potential (3.2.10) using this approximation becomes:

$$\frac{2m}{\hbar^2} \cdot V_{\Sigma}(r_{\Sigma}) \sim 4\pi \cdot A \left(1 + \frac{M_{\Sigma}}{M_N}\right) \left(\frac{\bar{a}}{1 + \bar{a}\mu/Q}\right) \int \underline{dr} f(\underline{r}_{\Sigma} - \underline{r}) \rho(\underline{r}). \quad (3.2.12)$$

Further, if the range of the potential is small in comparison with the nuclear dimensions, the integral can be written approximately as:

$$\int f(\underline{r}_{\Sigma} - \underline{r}) \rho(\underline{r}) \underline{dr} \approx \rho(r_{\Sigma}) \int f(\underline{r}_{\Sigma} - \underline{r}) \underline{dr} = \rho(r_{\Sigma}), \quad (3.2.13)$$

and therefore;

$$\frac{2m}{\hbar^2} \cdot V_{\Sigma}(r_{\Sigma}) \sim 4\pi A \left(1 + \frac{M_{\Sigma}}{M_N}\right) \left(\frac{\bar{a}}{1 + \bar{a}\mu/Q}\right) \cdot \rho(r_{\Sigma}). \quad (3.2.14)$$

In a first approximation the potential  $V_{\Sigma}$  is a non-linear function of the scattering length  $\bar{a}$ , and linear with the nuclear density. Only if the scattering length is small compared to the range  $\mu^{-1}$  does this expression reduce to the optical model.

The discrepancies in scattering length are attributable to making this assumption. Using an effective potential linear in the scattering length, Batty et al<sup>(1)</sup> determined the best



fitting depth parameter  $\bar{a}$  for  $\Sigma^-$  atoms to be:

$$\bar{a} = -0.35 \pm 0.04 - i0.19 \pm 0.03 \text{ fm.}$$

The zero-range approximation with  $a_{\Sigma N}$  values from Alexander et al<sup>(3)</sup> (Set (B)) predicts:

$$\bar{a} = \frac{1}{2}(a_{\Sigma p} + a_{\Sigma n}) = -0.05 - i0.49 \text{ fm.}$$

whereas the non-linear relationship with  $\mu/Q = 1$  gives:

$$\bar{a} = \frac{1}{2} \left( \frac{a_{\Sigma p}}{1 + a_{\Sigma p}} + \frac{a_{\Sigma n}}{1 + a_{\Sigma n}} \right) = -0.28 - i0.15 \text{ fm,}$$

in good agreement with the phenomenological value.

The non-linear relationship for  $V_{\Sigma}(r)$  is still only approximate and so it is worthwhile to return to the more general folding model (3.2.10) to describe the interaction. This expression has been used by Deloff and Law<sup>(9)</sup> and found, as expected, to give good agreement with experiment.

The disadvantage of this approach is that the description of the potential  $v$  appearing in the folding integral requires a knowledge of at least the depth and range. These parameters cannot both be determined unambiguously from the atomic level shift data alone, nor can the range be inferred directly from scattering length data. However, in this work both will be determined by requiring consistency of the atomic and scattering length data.

### 3.3: SPIN-DEPENDENT $\Sigma^-$ N POTENTIALS IN THE FOLDING MODEL

In the previous section the  $\Sigma^-$ -nucleus potential was developed assuming the two-body interactions to be identical in all  $\Sigma^-$ N channels. This restriction will now be removed and the weighting of spin-dependent potentials in the  $\Sigma^-$ -nucleus effective potential will be considered.

For the  $i^{\text{th}}$  nucleon in the nucleus, the  $\Sigma^-$ N potential may be written as:

$$V_{\Sigma N_i} = \left( \frac{3 + \underline{\sigma}_{\Sigma} \cdot \underline{\sigma}_i}{4} \right) \cdot V_{\Sigma N}^t + \left( \frac{1 - \underline{\sigma}_{\Sigma} \cdot \underline{\sigma}_i}{4} \right) \cdot V_{\Sigma N}^s, \quad (3.3.1)$$

where  $V_{\Sigma N}^t$  and  $V_{\Sigma N}^s$  are the  $\Sigma^-$ N spin triplet and singlet potentials respectively. N is the kind of nucleon, either n or p.  $\underline{\sigma}_{\Sigma}$  and  $\underline{\sigma}_i$  are the Pauli spin matrices of the  $\Sigma^-$  and N with the properties  $\underline{\sigma}_{\Sigma} \cdot \underline{\sigma}_i = -3$  for a singlet interaction and +1 for triplet interaction.

If the total nuclear angular momentum is J, then the expectation value of the  $\Sigma^-$ -nucleus potential is:

$$V_{\Sigma} = \langle J | \sum_{i=1}^{N,Z} \left( \frac{3V_{\Sigma N_i}^t + V_{\Sigma N_i}^s}{4} - \left( \frac{V_{\Sigma N_i}^s - V_{\Sigma N_i}^t}{4} \right) \underline{\sigma}_{\Sigma} \cdot \underline{\sigma}_i \right) | J \rangle, \quad (3.3.2)$$

where the summation is over all the nucleons. Evaluation of the above expression is dependent on the coupling scheme imagined for the nucleons. If it is supposed that each nucleon is in a state of definite total angular momentum  $j_i$ , then from the Wigner-Eckart theorem<sup>(20)</sup>, the expectation value of

the  $i^{\text{th}}$  nucleon spin may be written in terms of the angular momentum  $j_i$  as:

$$\langle j_i | \sigma_i | j_i \rangle = \langle j_i | j_i (\sigma_i \cdot j_i) | j_i \rangle / j_i (j_i + 1) . \quad (3.3.3)$$

Since  $j_i = \ell_i + \frac{\sigma_i}{2}$ , where  $\ell_i$  is the orbital angular momentum, this expression can immediately be put in a more tractable form by:

$$\begin{aligned} \langle j_i | j_i (\sigma_i \cdot \ell_i + \sigma_i \cdot \sigma_i / 2) | j_i \rangle / j_i (j_i + 1) \\ = \left( \frac{j_i (j_i + 1) - \ell_i (\ell_i + 1) + \frac{3}{4}}{j_i (j_i + 1)} \right) \langle j_i | j_i | j_i \rangle . \end{aligned} \quad (3.3.4)$$

In the summation of (3.3.2) this term gives zero contribution for nucleons of a closed shell or ground-state even-even nuclei since the total angular momentum  $J$  is zero.

In the coherent nucleus approximation all protons or neutrons outside a closed shell have the same  $j$  and  $\ell$  values so that the summation (3.3.2) becomes:

$$\begin{aligned} V_\Sigma = N \langle J | \left( \frac{3V_{\Sigma n}^t + V_{\Sigma n}^s}{4} \right) | J \rangle + Z \langle J | \left( \frac{3V_{\Sigma p}^t + V_{\Sigma p}^s}{4} \right) | J \rangle \\ - \alpha_n \cdot \langle J | \left( \frac{V_{\Sigma n}^s - V_{\Sigma n}^t}{4} \right) \sigma_{\Sigma n} \cdot J | J \rangle - \alpha_p \cdot \langle J | \left( \frac{V_{\Sigma p}^s - V_{\Sigma p}^t}{4} \right) \sigma_{\Sigma p} \cdot J | J \rangle , \end{aligned} \quad (3.3.5)$$

where

$$\alpha_N \equiv \left( \frac{j_N (j_N + 1) - \ell_N (\ell_N + 1) + \frac{3}{4}}{j_N (j_N + 1)} \right) , \quad (3.3.6)$$

where  $J_n, J_p$  denote the total angular momentum of the neutrons and protons respectively. Again, assuming that the  $\Sigma^-$  is in a state of definite angular momentum:

$$\begin{aligned}
 \langle J | \left( \frac{V_{\Sigma N}^s - V_{\Sigma N}^t}{4} \right) \sigma_{\Sigma} \cdot J_N | J \rangle &= \sum_{J'} \langle J | \left( \frac{V_{\Sigma N}^s - V_{\Sigma N}^t}{4} \right) | J' \rangle \langle J | \sigma_{\Sigma} \cdot J_N | J \rangle \\
 &= \langle J | \left( \frac{V_{\Sigma N}^s - V_{\Sigma N}^t}{4} \right) | J \rangle \cdot \delta_{JJ'} \cdot \beta_{\Sigma} \cdot \langle J | J_{\Sigma} \cdot J_N | J \rangle, \quad (3.3.7) \\
 &= \langle J | \left( \frac{V_{\Sigma N}^s - V_{\Sigma N}^t}{4} \right) | J \rangle \beta_{\Sigma} \cdot \frac{\gamma_{\Sigma N}}{2},
 \end{aligned}$$

where in the second line the coherent nucleus approximation has been used to decide that the states  $|J\rangle$  and  $|J'\rangle$  cannot be coupled by the potential for  $J \neq J'$ .

The constants  $\beta_{\Sigma}$  and  $\gamma_{\Sigma N}$  are defined as:

$$\beta_{\Sigma} \equiv \left( \frac{J_{\Sigma}(J_{\Sigma}+1) - l_{\Sigma}(l_{\Sigma}+1) + \frac{3}{4}}{J_{\Sigma}(J_{\Sigma}+1)} \right), \quad (3.3.8)$$

$$\gamma_{\Sigma N} \equiv (J_{\Sigma N}(J_{\Sigma N}+1) - J_N(J_N+1) - J_{\Sigma}(J_{\Sigma}+1)), \quad (3.3.9)$$

where  $J_{\Sigma}$ ,  $J_{\Sigma N}$  are the  $\Sigma^-$ , and total  $|J_{\Sigma} + J_N|$  angular momenta respectively. The effective potential  $V_{\Sigma}$  can now be written as

$$V_{\Sigma} = N \langle J | \left( \frac{3V_{\Sigma n}^t + V_{\Sigma n}^s}{4} \right) | J \rangle + Z \langle J | \left( \frac{3V_{\Sigma p}^t + V_{\Sigma p}^s}{4} \right) | J \rangle \quad (3.3.10)$$

$$- \alpha_n \beta_{\Sigma} \frac{\gamma_{\Sigma n}}{2} \langle J | \left( \frac{V_{\Sigma n}^s - V_{\Sigma n}^t}{4} \right) | J \rangle - \alpha_p \beta_{\Sigma} \frac{\gamma_{\Sigma p}}{2} \langle J | \left( \frac{V_{\Sigma p}^s - V_{\Sigma p}^t}{4} \right) | J \rangle.$$

This expression for the weighting of the  $\Sigma^-$ -N spin-dependent potentials in the  $\Sigma^-$ -nucleus potential will now be combined with the folding model of the last section.

For generality at this point, the neutron and proton density distributions will be kept separate and the ranges of the  $\Sigma^-n$  and  $\Sigma^-p$  potentials will be allowed to be different.

The two-body interaction is considered to be of the form:

$$v_{\Sigma N}^{s,t}(r) = v_{\Sigma N}^{s,t} \cdot f_{\Sigma N}(r), \quad (3.3.11)$$

where  $v_{\Sigma N}^{s,t}$  is the complex depth parameter and  $f_{\Sigma N}(r)$  is the smooth functional form of the interaction.

Combining (3.3.10) with (3.2.10) of the last section gives the general  $\Sigma^-$ -nucleus potential in the form:

$$V_{\Sigma} = N \left( \frac{3V_{\Sigma n}^t + V_{\Sigma n}^s}{4} \right) \int d\mathbf{r} f_{\Sigma n}(\mathbf{r}_{\Sigma} - \mathbf{r}) \rho_n(\mathbf{r}) + Z \left( \frac{3V_{\Sigma p}^t + V_{\Sigma p}^s}{4} \right) \int d\mathbf{r} f_{\Sigma p}(\mathbf{r}_{\Sigma} - \mathbf{r}) \rho_p(\mathbf{r}) \\ - \alpha_n \beta_{\Sigma} \frac{\gamma_{\Sigma n}}{2} \left( \frac{V_{\Sigma n}^s - V_{\Sigma n}^t}{4} \right) \int d\mathbf{r} f_{\Sigma n}(\mathbf{r}_{\Sigma} - \mathbf{r}) \rho_n(\mathbf{r}) \quad (3.3.12) \\ - \alpha_p \beta_{\Sigma} \frac{\gamma_{\Sigma p}}{2} \left( \frac{V_{\Sigma p}^s - V_{\Sigma p}^t}{4} \right) \int d\mathbf{r} f_{\Sigma p}(\mathbf{r}_{\Sigma} - \mathbf{r}) \rho_p(\mathbf{r}).$$

In a first approximation the nucleon densities are considered to be the same, and the functional forms  $f_{\Sigma n}$  and  $f_{\Sigma p}$  are the same.

Further, in most cases of interest the 'correction' terms in  $\alpha\beta\gamma$  give zero contribution because the nuclei involved are even-even<sup>(1,9)</sup>. In the event of an odd number of nucleons these corrections are found to affect the calculated complex shifts by less than 5%.

Making these approximations gives a simple expression for the  $\Sigma^-$ -nucleus potential as:

$$V_{\Sigma} = (N \cdot \left( \frac{3V_{\Sigma n}^t + V_{\Sigma n}^s}{4} \right) + Z \cdot \left( \frac{3V_{\Sigma p}^t + V_{\Sigma p}^s}{4} \right)) \cdot \int d\mathbf{r} f_{\Sigma N}(\mathbf{r}_{\Sigma} - \mathbf{r}) \rho(\mathbf{r}) ,$$

(3.3.13)

$$\equiv V_{\Sigma N}^0 \cdot \int d\mathbf{r} f_{\Sigma N}(\mathbf{r}_{\Sigma} - \mathbf{r}) \rho(\mathbf{r}) .$$

This last, simplest form for the potential is used throughout this work and is found adequate to predict the atomic complex level shifts.

#### 3.4: COMPLEX LEVEL SHIFTS DETERMINED FROM THE SCHRÖDINGER EQUATION

With the development in the previous sections of an expression for the  $\Sigma^-$ -nucleus strong interaction it is now possible to determine the complex shifts predicted by the Schrodinger equation.

The complex energy shift  $\delta E$  is defined as the difference:

$$\delta E \equiv E - E_0 = - (\epsilon + i\Gamma/2) , \quad (3.4.1)$$

where  $E$  and  $E_0$  are the energy eigenvalues of the level  $(n, \ell)$  with and without the strong interaction. Because  $\delta E$  is defined as the difference between two binding energies, all electromagnetic corrections such as finite-size effects and vacuum polarization cancel and need not be included in the Schrodinger equation<sup>(9)</sup>.

The radial equation for the  $\Sigma^-$ -nucleus system then becomes:

$$\psi_{\Sigma}''(k, r) + \left( k^2 + \frac{2mc}{\hbar} \frac{\alpha Z}{r} - \frac{\ell(\ell+1)}{r^2} - \frac{2m}{\hbar} V_{\Sigma}(r) \right) \psi_{\Sigma}(k, r) = 0 , \quad (3.4.2)$$

where  $Z$  is the nuclear charge,  $\alpha$  the fine-structure constant,  $k$  the complex wavenumber of the quasi-bound state, and  $V_{\Sigma}(r)$  the  $\Sigma^-$ -nucleus strong interaction.

The method given here for calculating  $\epsilon$  and  $\Gamma$  from (3.4.2) is adapted from Deloff's procedure<sup>(14,15)</sup> and based on a Newton-Raphson iterative scheme for  $\delta E$ . Details of the derivation of the complex shift equation are given in Appendix B. Deloff shows though, that for the circular orbits, the shift  $\delta E$  is approximately given by:

$$\delta E = -\frac{\pi^2}{2m} e^{2ik_0 R} \cdot (-2ik_0 R)^{2\ell+3} \left( R \frac{\phi'(k_0, R)}{\phi(k_0, R)} - \ell(\ell+1) - ik_0 R \right) / R^2 \Gamma(2\ell+3). \quad (3.4.3)$$

In deriving this expression, it is assumed that for some large distance  $R$  the strong interaction is essentially zero. The  $\phi(k_0, r)$  is the regular hadron wavefunction evaluated from the radial equation (3.4.2) but with the approximation that the true binding energy is replaced by the unperturbed Coulomb energy  $k_0$ .

The above expression (3.4.3) is only an approximate solution for  $\delta E$ , as it represents only the first iteration of the Newton-Raphson algorithm. Nonetheless, the equation has been tested extensively by Deloff<sup>(15)</sup> and found to give results accurate within 4% of the true shift determined from a full solution of the complex, bound-state problem.

This formula together with the previous results derived in this chapter provide a firm basis for determining the  $\Sigma$ -atom complex shifts. Specification of the  $\Sigma N$  two-body potentials allows calculation of the  $\Sigma$ -nucleus interaction via the folding model with the potential spin-dependence accounted for by the weighting prescription.

Rapid numerical determination of the complex shift is possible by a single iteration of the radial Schrodinger equation for the perturbed  $\Sigma$  wavefunctions.

In this work, the two-body potentials which enter the folding model are those which are consistent with the  $\Sigma N$



scattering lengths. It is therefore possible to correlate the scattering and atomic data and extract optimum  $\Sigma N$  effective potentials.

## CHAPTER 4

### ΣN POTENTIAL OPTIMIZATION

#### 4.1: SCATTERING LENGTH CALCULATIONS

The scattering lengths of Alexander et al<sup>(3)</sup> were derived from  $\Sigma^+$  proton scattering. These results can be related to the  $\Sigma^-n$  potentials by noting that the  $\Sigma^+p$  and  $\Sigma^-n$  systems are both pure  $I = \frac{3}{2}$  states. Consequently, the  $\Sigma^-N$  and  $\Sigma^+p$  strong interactions, and therefore scattering lengths, are identical, assuming the force to be charge invariant. There are several reasons why this symmetry is not expected to be exact. The  $\Sigma^+$  mass difference of 8 Mev will affect the magnitude of the strong interaction, and in addition, there are uncertainties in the  $\Sigma^+p$  scattering lengths arising from the approximations used in introducing the Coulomb effect to the cross-sections.

Nonetheless, the errors in the data of Alexander (Table 4.1) are large enough to make the symmetry an adequate approximation for the purposes of this work.

An additional approximation of the  $\Sigma^-p$  scattering lengths is used in this study. The scattering lengths as listed by Alexander consider the  $\Sigma^-p$  interactions in each separate I,J channel which is not a convenient form for the

present analysis. To arrive at  $\Sigma^- p$  potentials which are compatible with the spin-weighting prescription (3.1.13), a method for averaging the  $I = \frac{1}{2}, \frac{3}{2}$  channels in the  $\Sigma^- p$  interactions is required.

The  $|\Sigma^- p\rangle$  wavefunction was expanded in isospin states in section 2.1 with the result:

$$|\Sigma^- p\rangle = \sqrt{\frac{1}{3}} \left| \frac{3}{2} - \frac{1}{2} \right\rangle + \sqrt{\frac{2}{3}} \left| \frac{1}{2} - \frac{1}{2} \right\rangle, \quad (4.1.1)$$

which indicates, from the squares of the Clebsch-Gordan coefficients, that the  $\Sigma^- p$  interaction occurs  $\frac{1}{3}$  of the time in the  $I = \frac{3}{2}$  channel and  $\frac{2}{3}$  in the  $I = \frac{1}{2}$ . This information can be applied to the measured scattering lengths. If the  $\Sigma^- p$  is in a definite spin-state of total angular momentum  $J$ , then the corresponding scattering length can be written as:

$$a_J = \left( \frac{2 + \tau_{\Sigma} \cdot \tau_p}{3} \right) a_{J3/2} + \left( \frac{1 - \tau_{\Sigma} \cdot \tau_p}{3} \right) a_{J1/2}, \quad (4.1.2)$$

here the coefficients for the  $a_{JI}$  are isospin projection operators. For the  $\Sigma^- p$  system,  $\tau_{\Sigma} \cdot \tau_p = +1$  and  $-2$  for  $I = \frac{3}{2}$  and  $\frac{1}{2}$  respectively. Equivalently, (4.1.2) can be re-arranged into the form:

$$a_J = \frac{1}{3} (2a_{J3/2} + a_{J1/2}) + \frac{1}{3} (a_{J3/2} - a_{J1/2}) \tau_{\Sigma} \cdot \tau_p. \quad (4.1.3)$$

At low energies (long wavelength) the  $\Sigma^-$  interacts with more than one proton scattering centre concurrently. Ultimately,

in the  $k \rightarrow 0$  limit; the term  $\tau_{\Sigma} \cdot \tau_{\bar{p}}$  can be replaced by an average value. Recalling the probability of interaction in a given isospin state, and the corresponding value of  $\tau_{\Sigma} \cdot \tau_{\bar{p}}$ , this average is:

$$\langle \tau_{\Sigma} \cdot \tau_{\bar{p}} \rangle = \frac{2}{3}(-2) + \frac{1}{3}(1) = -1. \quad (4.1.4)$$

Substituting this result into (4.1.3) gives the isospin-averaged scattering length in the spin state  $J$  as:

$$a_J = \frac{1}{3} a_{J3/2} + \frac{2}{3} a_{J1/2}. \quad (4.1.5)$$

This last expression is only strictly valid in the zero-energy limit. In consequence, the two-body potential which reproduces the average  $a_J$  becomes only approximately correct in describing the  $\Sigma^{-}p$  interaction when used in the  $\Sigma$ -nucleus potential folding model.

Since the  $\Sigma^{-}$ -nucleus interaction occurs at low energies though, the discrepancy is expected to be small.

With the acceptance of the last two assumptions concerning  $\Sigma^{-}n$  and  $\Sigma^{-}p$  scattering lengths, a method is required for calculating the scattering lengths as a function of the potential strength. Two distinct methods are used in this work with the first, and most obvious, being numerical solution of the Schrodinger equation at zero energy. Coulomb interaction is neglected in this calculation since the extracted scattering lengths are supposed to arise only from the strong

interaction. For some large separation  $R$ , such that the potential is zero essentially for  $r \geq R$ , the logarithmic derivative of the wavefunction evaluated at zero energy, is simply related to the scattering length by:

$$a = R - \frac{\phi(0, R)}{\phi'(0, R)} \quad (4.1.6)$$

The potential dependence of the scattering length enters through the value of the wavefunction. Conversely, if the scattering length is known, as is the case here, a method is needed for determining the correct potential. A Newton-Raphson iterative procedure is developed in Appendix A for determining the potential strength assuming the range is fixed. It is shown that the first order correction  $\Delta V$  to the initial guess of the strength  $V_I$  is:

$$\Delta V = \left( a - R + \frac{\phi(0, R)}{\phi'(0, R)} \right) \frac{\hbar^2}{2m} (\phi'(0, R))^2 \int_0^R \phi^2(0, r) f(r) dr, \quad (4.1.7)$$

with  $f(r)$  the shape of the potential. By setting the depth  $V = V_I + \Delta V$ , and repeating the iteration, the depth converges quadratically to the root  $V_0$ . This procedure can be as accurate as desired but its one drawback is that it requires solving the radial equation numerically from  $r = 0 \rightarrow R$ . This can involve evaluation of the wavefunction at hundreds of steps.

An alternative method is one developed by Deloff<sup>(17)</sup>. In his work the scattering length is related to the potential

depth and range by an infinite product representation:

$$a = sC \prod_n \frac{1 - (S/Z_n)}{1 - (S/S_n)} \quad (4.1.8)$$

where  $S$  is a constant involving the potential depth and range;  $C$ ,  $S_n$ , and  $Z_n$  are constants dependent on the potential shape. The values of these for the Yukawa potential are given in the computer program of Appendix C. Other simple potential forms are in the original work. Equation (4.1.8) converges rapidly and the first three or four terms of the expansion are sufficient to achieve four figure accuracy.

The numerical advantages of such an expression are clear. Solving the complete Schrodinger equation, and the calculation of four algebraic terms result in equivalent accuracy of the scattering length.

For the case of a known scattering length and unknown potential strength it is straightforward to invert equation (4.1.8) to solve for the depth  $V_0$ . Inversion of the two leading terms has been found to be accurate within a few per cent.

It may be clear from the infinite product representation that it is not necessarily true that there is a unique potential depth for each scattering length. Depending on whether the scattering length is real or complex, and whether  $\text{Re}(a)$  is greater or less than zero, the number of potential depths and characteristics can be classified as follows:

Re(a)	Real a Potentials	Re(v)	Potentials	Complex a Re(v)
<0	1	--weak attraction	2	- weak attraction
				- strong attraction
>0	2	- strong attraction with bound state - repulsion	4	- weak attraction
				- strong attraction
				- weak repulsion - strong repulsion

This table can now be compared with Alexander's data. Using the isospin averaging procedure and the equivalence of the  $\Sigma^-n$  and  $\Sigma^-p$  interactions, his two possible scattering length sets are shown in Table 4.1.

	Set (1)		Set (2)	
	Re(a)	Im(a)	Re(a)	Im(a)
$\Sigma^-n$ (S=0)	$-1.40 \pm 1.30$	0.	$0.80 \pm 2.00$	0.
$\Sigma^-n$ (S=1)	$0.70 \pm 0.40$	0.	$0.80 \pm 0.70$	0.
$\Sigma^-p$ (S=0)	$0.40 \pm 0.90$	$-0.53 \pm 0.60$	$-0.60 \pm 1.68$	$-1.00 \pm 1.83$
$\Sigma^-p$ (S=1)	$-0.50 \pm 0.47$	$-1.13 \pm 0.53$	$-0.60 \pm 0.57$	$-1.00 \pm 0.93$

TABLE 4.1.  $\Sigma N$  SCATTERING LENGTHS (FM) ADAPTED FROM ALEXANDER ET.AL. (3).

From the above discussion of potential depths it is evident there is a great deal of ambiguity connected with the potentials producing these scattering lengths. In fact there are

16 possible combinations of potentials for each scattering length set.

Not all 32 combinations are used in the present work. The main criteria in discarding possible sets is the requirement that all potential strengths within a combination be roughly the same magnitude. This is not unreasonable in consideration of the NN interactions where the potentials are approximately the same in all states. However, in those states with positive scattering lengths, both strongly attractive and repulsive potential possibilities are used. In this way, eventually three different combinations for each scattering length set are fitted to the  $\Sigma$  atom data.

#### 4.2: $\Sigma$ ATOM COMPLEX SHIFT CALCULATIONS

In calculating the  $\Sigma$  atom complex energy shifts, several simplifying approximations are made. It is assumed that the Schrodinger, rather than Dirac, equation is adequate for describing the  $\Sigma$  atom system. The error introduced in the shifts by not treating the problem relativistically is estimated to be of the order of 2-3 %, which is small in comparison with the large experimental uncertainties. Secondly, the neutron and proton density distributions are considered to be identical and described by the Woods-Saxon form. Further, to minimize the number of parameters, the ranges of the two-body potentials are kept the same for all  $\Sigma N$  states. In



this way the folding model reduces to one shape for all interaction channels.

For the Yukawa potential and spherically symmetric density, the  $\Sigma^-$ -nucleus folding model becomes:

$$\int dr \rho(r) \frac{e^{-\mu|r_{\Sigma}-r|}}{\mu|r_{\Sigma}-r|} = \frac{2\pi}{\mu^2 r_{\Sigma}} \int_0^{\infty} dr r^2 \rho(r) \left( e^{-\mu|r_{\Sigma}-r|} - e^{-\mu(r_{\Sigma}+r)} \right) \quad (4.2.1)$$

The complete  $\Sigma$ -nucleus potential for a Woods-Saxon density is then:

$$V_{\Sigma}(r_{\Sigma}) = V_{\Sigma N}^0 \frac{2\pi}{\mu^2 r_{\Sigma}} \rho_0 \int_0^{\infty} dr r^2 \left( \frac{e^{-\mu|r_{\Sigma}-r|} - e^{-\mu(r_{\Sigma}+r)}}{1 + \exp((r-c)/a)} \right) \quad (4.2.2)$$

with

$$V_{\Sigma N}^0 \equiv N \left( \frac{3V_{\Sigma n}^t + V_{\Sigma n}^s}{4} \right) + Z \left( \frac{3V_{\Sigma p}^t + V_{\Sigma p}^s}{4} \right) \quad (4.2.3)$$

and

$$\rho_0 = \frac{3}{4\pi c^3} \left( 1 + \left( \frac{\pi a}{c} \right)^2 \right)^{-1} \quad (4.2.4)$$

This is the final expression for the  $\Sigma$ -nucleus effective potential. The integral is non-analytic and must be evaluated numerically for each value of  $r_{\Sigma}$ . The constants  $c$  and  $a$  appearing in the density expression are the nuclear half-density radius and skin thickness respectively (see refs. 27 and 28).

Specification of the  $\Sigma N$  potential depths and range completely determines the  $\Sigma$ -nucleus interaction. This expression for  $V_{\Sigma}$  is then inserted in the radial equation (3.4.2). Numerically solving the equation for the wavefunction and its deriva-

tive determines the complex shift (equations (3.4.3) and (B.12) to be:

$$\delta E = -\frac{\hbar^2}{2m} e^{2ik_0 R} (-2ik_0 R)^{2\ell+3} \left( R \frac{\phi'(k_0, R)}{\phi(k_0, R)} - \ell(\ell+1) - ik_0 R \right) / R^2 \Gamma(2\ell+3). \quad (4.2.5)$$

The  $\Sigma^-$  atom data available are very scarce and the only complete measurements of the complex energy shifts are those of Batty et al<sup>(1)</sup>. Their results are shown below in Table 4.2.

Element	Transition n+1+n	$\epsilon_n$	$\Gamma_n$ (eV)	$\Gamma_{n+1}$
O	4+3	320±230	-	.98 <sup>+1.68</sup> -0.44
Mg	5+4	25±40	<70	.11 <sup>+0.10</sup> -0.07
Al	5+4	68±28	43±75	.25 <sup>+0.06</sup> -0.05
Si	5+4	159±36	217±110	.41 <sup>+0.11</sup> -0.09
S	5+4	360±220	870±700	1.47 <sup>+1.01</sup> -0.56

TABLE 4.2  $\Sigma$  ATOM COMPLEX ENERGY SHIFTS (1).

Some slightly older data are available from H. Koch<sup>(2)</sup> who measured the upper level widths in four atoms. His results are listed below in Table 4.3.

Element	Transition n+1→n	$\Gamma_{n+1}$ (eV)
C	4→3	.031±.012
Ca	6→5	.40 ±.22
Ti	6→5	.66 ±.43
Ba	8→7	1.68 ±3.60

TABLE 4.3  $\Sigma$  ATOM UPPER LEVEL WIDTHS  
(2)

The widths alone are not enough to determine unambiguously a complex potential depth, as the effects of the real and imaginary components are coupled. Nonetheless, these data can be included with the more complete results of Batty.

Although these widths are not used in the  $\chi^2$  minimization procedure of the next section, the predicted shifts of the optimized  $\Sigma N$  potentials are compared with Koch's values.

The complex atomic energy shifts are connected with the scattering lengths through the two-body potentials entering equation (4.2.2) for the  $\Sigma$ -nucleus effective interaction. Since both  $a$  and  $\delta E$  depend on the  $\Sigma N$  potential depths and range, the potential parameters can be determined by optimizing the fit to all the scattering and atomic data.

### 4.3 POTENTIAL OPTIMIZATION CALCULATIONS

It is clear from the discussions of the last two sections that the problem of extracting consistent  $\Sigma N$  potentials is not straightforward. Difficulties arise from the large number of potential sets possible, and the few pieces of data available for the fitting procedure.

As mentioned earlier, eventually all but six potential combinations were eliminated. The distinct natures of the remaining potentials are summarized below.

Set (1)	Potentials				
	Re(a)	Im(a)	A	B	C
$\Sigma^-_n(S=0)$	-1.40	0.			
$\Sigma^-_n(S=0)$	0.70	0.	strong attraction	repulsion	repulsion
$\Sigma^-_p(S=0)$	0.40	-0.53	strong attraction	strong attraction	repulsion
$\Sigma^-_p(S=1)$	-0.50	-1.13			
Set (2)	Potentials				
	Re(a)	Im(a)	A	B	C
$\Sigma^-_n(S=0)$	0.80	0.	strong attraction	strong attraction	repulsion
$\Sigma^-_n(S=1)$	0.80	0.	strong attraction	repulsion	repulsion
$\Sigma^-_p(S=0)$	-0.60	-1.00			
$\Sigma^-_p(S=1)$	-0.60	-1.00			

TABLE 4.4 POTENTIAL COMBINATIONS FOR SCATTERING LENGTHS

Complex-Yukawa-shaped potentials were assumed to describe the  $\Sigma N$  interactions:

$$V_{\Sigma N}(r) = V_{JI} \frac{e^{-\mu r}}{\mu r} \quad (4.3.1)$$

The complex depths were fixed to fit the central values of the scattering lengths in sets (1) and (2) of Table 4.1 using the iterative approach of Appendix A. By varying  $\mu$  over a wide range, and repeating the above procedure, the depths were determined as a function of the inverse range  $\mu$ .

Folding the resulting two-body potentials into the nuclear distributions of the  $\Sigma$  atoms (Table 4.2) produced the  $\Sigma$ -nucleus potentials (4.2.2). Solving the radial equation with these potentials predicted the atomic complex shifts, using equation (4.2.5) for  $\delta E$ .

This calculation was repeated for each value of the inverse range  $\mu$  and corresponding depths to determine the minimum  $\chi^2$  of the fit to the atomic data as a function of  $\mu$ .

Because of the large errors in the scattering data it is not reasonable to limit the potential strengths to values which exactly reproduce the scattering lengths. It was decided then to treat all six depth parameters and range as variables.

Using the minimum in the curve of  $\chi^2$  as a function of  $\mu$  as a starting point, the total  $\chi^2$  to all the atomic and

scattering data was then minimized by varying all seven potential parameters. This is a long process since the real and imaginary components of the potential are coupled in their effects, with the result that the  $\chi^2$  can not be minimized with respect to each parameter independently and therefore an iterative solution is required. To decrease computing time, the scattering lengths were calculated in this optimization program using the infinite product representation (4.1.8). The computer program used to perform this minimization is listed and commented in Appendix C.

This approach was used for all six potential combinations which produced six minima in the  $\chi^2$  hypersurface. The resulting best-fitting potentials all produce a total  $\chi^2$  on the order of 10 for sixteen degrees of freedom. On this basis then the  $\chi^2$  alone can not distinguish between the six potential sets.

Nonetheless, four of these solutions will be seen to be unacceptable, so they will be discussed first. The optimized potentials A and B for sets (1) and (2) of Table 4.4 are reproduced in Table 4.5. These are the four sets for which a positive scattering length has been interpreted as a bound state.

	Potential Depths (Mev)							
	Set (1)				Set (2)			
	A		B		A		B	
	Re(v)	Im(v)	Re(v)	Im(v)	Re(v)	Im(v)	Re(v)	Im(v)
$\Sigma^-_n(S=0)$	-179.3	0.	-88.9	0.	-747.2	0.	-207.3	0.
$\Sigma^-_n(S=1)$	-544.4	0.	150.8	0.	-612.6	0.	90.4	0.
$\Sigma^-_p(S=0)$	-751.3	-744.9	-320.6	-4.8	-180.8	-211.0	-36.3	-7.7
$\Sigma^-_p(S=1)$	-180.9	-103.5	-77.1	-39.9	-188.0	-105.0	-33.9	-11.6
$\mu(\text{fm}^{-1}) =$	2.04		1.52		2.13		1.23	

TABLE 4.5 BEST-FITTING POTENTIALS A, B OF SETS (1) AND (2).

In all four of the above sets, at least one of the states predicts an unrealistically large binding energy. The A solutions of sets (1) and (2) give  $\Sigma^-_n$  binding in the neighbourhood of 110 Mev. B of set (2) predicts a  $\Sigma^-_n$  bound state at 50 Mev and even the real part of the  $\Sigma^-_p$   $^1S_0$  potential of B, set (1) would bind the  $\Sigma^-_p$  with 82 Mev, or more instructively, this is about 4 Mev larger than the  $\Sigma\Lambda$  mass difference. This implies that the  $\Sigma p \rightarrow \Lambda n$  decay would be energetically unfavourable. As discussed earlier in this work, these huge binding energies are not impossible but they are highly improbable. For this reason the four solutions are all discarded.

Results of the optimization procedure for the remaining two solutions are shown in Tables 4.6 and 4.7 where their predictions are compared with the experimental findings of Alexander, Batty and Koch.

SCATTERING LENGTH (fm)	EXPERIMENTAL				CALCULATED				POTENTIAL DEPTH			
	SET (1)		SET (2)		SET (1)		SET (2)		SET (1)		SET (2)	
	Re(a)	Im(a)	Re(a)	Im(a)	Re(a)	Im(a)	Re(a)	Im(a)	Re(V)	Im(V)	Re(V)	Im(V)
$\Gamma_n^-(s=0)$	-1.4±1.3	0.	0.8±2.0	0.	-1.70	0.	-0.07	0.	-51.24	0.	-5.55	0.
$\Gamma_n^-(s=1)$	0.7±0.4	0.	0.8±0.7	0.	0.32	0.	0.31	0.	24.82	0.	31.32	0.
$\Sigma_p^-(s=0)$	0.4±0.9	-0.3±0.6	-0.6±1.7	-1.0±1.8	0.15	-0.11	-1.00	-0.42	9.81	-8.32	-30.11	-11.16
$\Sigma_p^-(s=1)$	-0.3±0.3	-1.1±0.5	-0.6±0.6	-1.0±0.9	-0.75	-0.48	-0.81	-0.66	-35.30	-13.04	-48.11	-19.61
SCATTERING $\chi^2$					3.36		0.66					

TABLE 4.6 SCATTERING LENGTHS AND POTENTIAL DEPTHS (Mev) FOR BEST FIT TO DATA WITH  $\mu$  1.20 and 1.30 fm<sup>-1</sup>. FOR SET (1) AND (2) RESPECTIVELY.

ELEMENT	TRANSITION	EXPERIMENTAL			CALCULATED					
		n+1-n	$\Gamma_n$	$\Gamma_{n+1}$	SET (1)			SET (2)		
			(eV)		$\Gamma_n$	$\Gamma_{n+1}$	$\Gamma_n$	$\Gamma_{n+1}$	$\Gamma_n$	$\Gamma_{n+1}$
C	4-3	-	-	0.031±0.012	24.2	17.6	0.020	25.1	18.9	0.018
O	4-3	320±230	-	0.98 <sup>+1.68</sup> <sub>-0.44</sub>	212.8	171.4	0.313	222.5	189.7	0.297
Nq	5-4	25±40	70	0.11 <sup>+0.10</sup> <sub>-0.07</sub>	35.1	25.3	0.087	35.8	26.4	0.082
Al	5-4	68±38	43±75	0.24 <sup>+0.06</sup> <sub>-0.05</sub>	64.9	49.1	0.187	62.9	51.1	0.173
Si	5-4	159±36	217±10	0.41 <sup>+0.11</sup> <sub>-0.09</sub>	143.9	108.4	0.504	148.6	116.2	0.483
P	5-4	-	-	-	258.3	205.0	1.061	256.7	219.7	1.019
S	5-4	360±220	870±700	1.47 <sup>+1.01</sup> <sub>-0.56</sub>	480.8	385.1	2.295	502.5	424.0	2.245
Ca	6-5	-	-	0.40±0.22	37.5	26.8	0.181	37.2	27.2	0.165
Tl	6-5	-	-	0.66±0.43	96.9	75.2	0.616	86.7	76.3	0.568
Ba	8-7	-	-	1.68±1.60	49.4	40.5	0.930	33.1	38.1	0.806
ATOMIC $\chi^2$					6.71			6.99		
TOTAL $\chi^2$					10.07			8.10		

TABLE 4.7 BEST FITS TO THE LEVEL WIDTHS AND SHIFTS CONSISTENT WITH THE SCATTERING DATA.



The total  $\chi^2$  of the fits are 10.1 and 8.1 for scattering length sets (1) and (2) respectively. Set (2) seems to be favoured, and comparison of the results indicates that the difference is due mainly to the contribution from the scattering lengths, whereas the  $\Sigma$  atomic  $\chi^2$  are almost insensitive to the differences between the sets.

The resultant fits to Batty's data are shown in figure 4.1 for the  $5 \rightarrow 4$  transition atoms. In addition, the  $\Sigma^-p$  scattering differential cross-sections predicted by the sets are shown in figure 4.2 again indicating that set (2) is the better fit.

The important point is that both sets favour a weak repulsive  $\Sigma^-n$   $^3S_1$  interaction rather than strong attraction, and the overall indication is that the  $\Sigma N$  potentials are weak relative to the NN interactions.

#### 4.4 $\Sigma$ HYPERNUCLEI

$\Sigma$  hypernuclei could be produced through the strangeness-exchange reaction  $K^- + N \rightarrow \Sigma^- + \pi$ , in exposing a nuclear target to low momentum  $K^-$  beams. It is not generally expected though that the  $\Sigma$  hypernucleus would exist long enough to identify because of the strong  $\Sigma^-p$  decay. However, if the width  $\Gamma$  of the  $\Sigma$  energy level was small, there would be some hope of detecting them.

The two acceptable potential sets of the last section

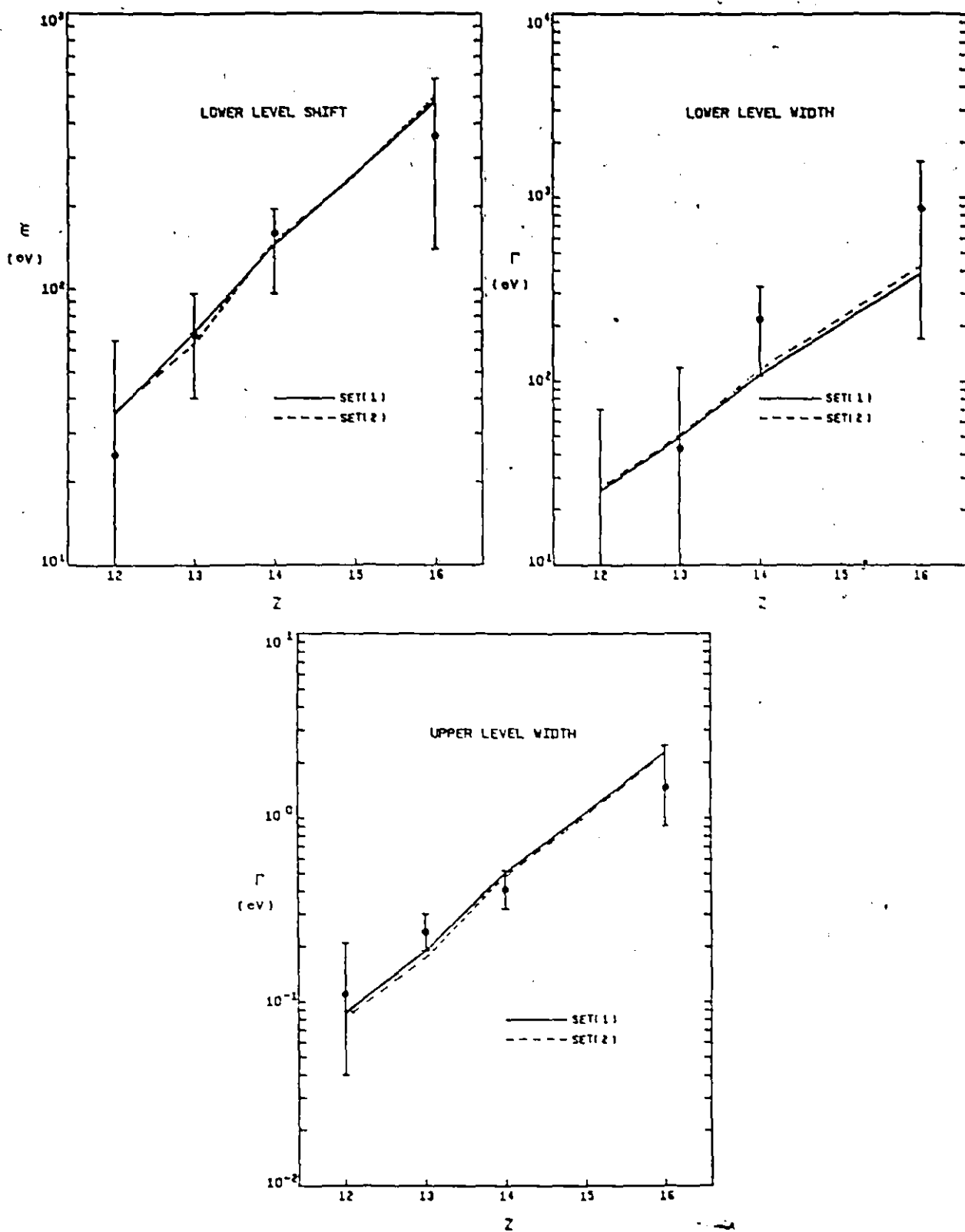


FIG. 4.1.

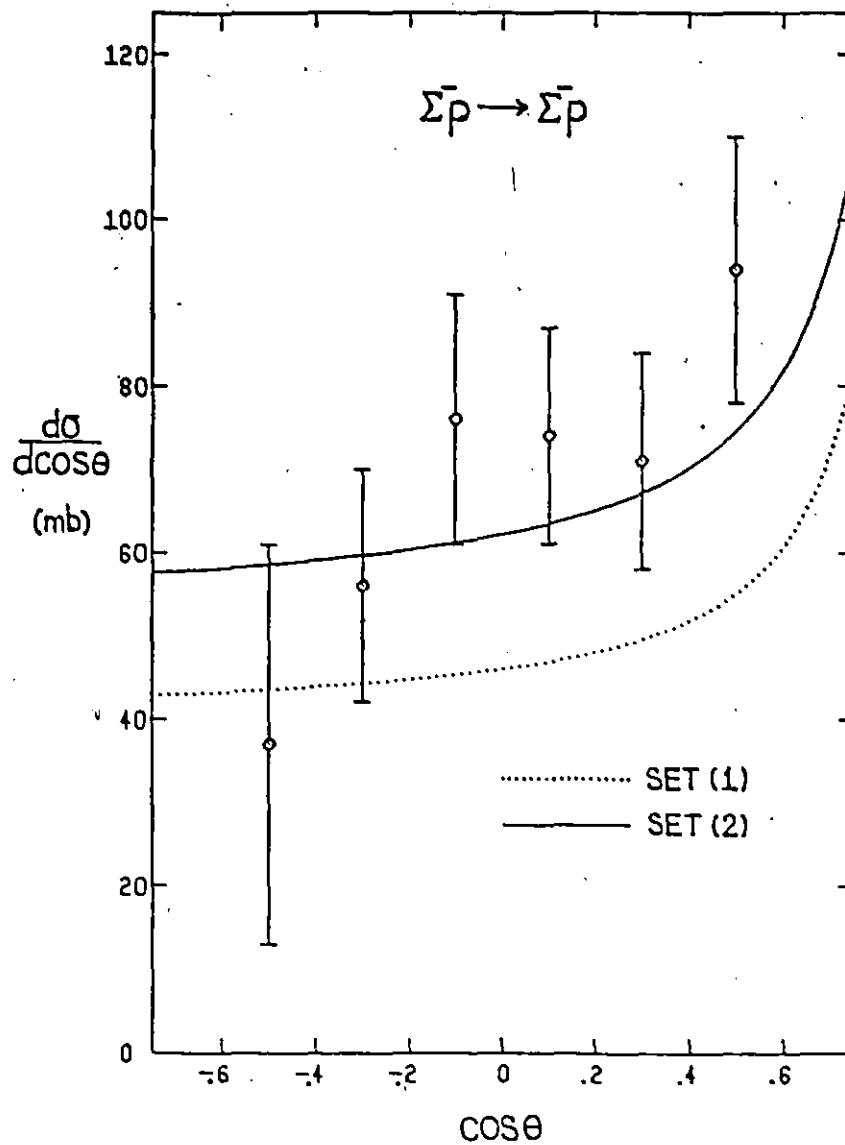


FIG. 4.2. ELASTIC  $\Sigma^- p$  DIFFERENTIAL CROSS-SECTION

are used here to predict the complex, ground state binding energy in a few proposed hypernuclei. The nuclei have been chosen so as to scan the periodic table.

The method of solution is straightforward and completely analogous to the procedure used for the  $\Sigma$  atoms.  $\Sigma$ -strong and Coulomb potentials are folded into the nuclear density distribution to produce the effective  $\Sigma$ -nucleus potential. With this potential the Schrodinger equation is solved numerically to determine the  $\Sigma^-$  complex ground state energy.

Results for this procedure for four nuclei are shown in Table 4.8.

Nucleus	$\Sigma$ Binding Energy			
	Set (1) Re(E)	Set (1) Im(E)	(Mev) Re(E)	Set (2) Im(E)
$^{12}\text{C}$	1.85	1.52	2.19	2.12
$^{16}\text{O}$	3.49	2.58	4.25	3.42
$^{40}\text{Ca}$	10.48	4.33	11.65	5.30
$^{208}\text{Pb}$	27.24	5.32	25.74	6.16

TABLE 4.8 PREDICTED  $\Sigma$  HYPERNUCLEI BINDING ENERGIES.

It is clear from the table that  $\Sigma$  hypernuclei are not likely to be seen, as expected. The lifetime of the bound  $\Sigma$  in  $^{16}\text{O}$  for example is predicted to be  $\tau = \hbar/\Gamma \sim 10^{-22}$  secs. This is a factor of  $10^3$  shorter than in the  $\Sigma$  atoms, which makes the  $\Sigma$  hypernucleus existence improbable.

CHAPTER 5  
CONCLUSIONS

It has been shown that the optimum  $\Sigma N$  parameters consistent with both the atomic and scattering data indicate there is a repulsive interaction in the  $\Sigma^- n \ ^3S_1$  state. This unusual result deserves further consideration. In the one-boson exchange model the  $\Sigma N$  potential is:

$$V(\text{OBE}) = \frac{g_\Sigma g_N}{12M_\Sigma M_N} \cdot \mu^3 (\tau_\Sigma \cdot \tau_N) (\sigma_\Sigma \cdot \sigma_N) \frac{e^{-\mu r}}{\mu r} \quad (5.1)$$

where the tensor component has been neglected since it gives zero average contribution in S state. The values of the coupling constants are not important for this discussion, except for the fact that they are both positive. Whether the potential is attractive or repulsive is then completely determined by the spin and isospin terms.

For the pure  $I = \frac{3}{2}$   $\Sigma^- n$  interaction  $\tau_\Sigma \cdot \tau_n = +1$ , and the spin term  $\sigma_\Sigma \cdot \sigma_n = -3$  and  $+1$  for the singlet and triple states respectively. Therefore it is predicted by the OBE model that, in the long-range tail of the potential at least, the  $\Sigma^- n$  interaction should be repulsive in the spin-triplet states, in agreement with the results of this work.

Further, both sets of potentials predict weakly attractive  $\Sigma^- n$  singlet potentials. These interactions are too weak

to support a  $\Sigma^-n$  bound state and, since the triplet potential is repulsive, it follows that the  $\Sigma^-nn$  system is also unbound.

To summarize the findings of this study then; it is found that the scattering and atomic data can be fitted in a consistent manner but because of the large experimental uncertainties, it is not yet possible to conclusively distinguish between the two sets of scattering lengths. However, both sets of extracted potentials predict that neither the  $\Sigma^-n$ , nor  $\Sigma^-nn$  bound states exists.

The overall indications are that the  $\Sigma N$  interactions are weak relative to NN interactions, and more importantly the  $\Sigma^-n$  triplet potential is almost certainly repulsive.

## APPENDIX A

ITERATIVE SOLUTION TO POTENTIAL FOR KNOWN  
SCATTERING LENGTH

The iterative procedure developed here is a Newton-Raphson algorithm for determining the potential depth  $V_0$  corresponding to a known scattering length  $a$ . It is assumed that the potential can be written in the form:

$$V(r) = V_0 f(r) , \quad (\text{A.1})$$

where  $V_0$  is the potential strength and  $f(r)$  is a smooth function of  $r$ . The potential is also considered to be short-ranged so that for some value  $R$  the potential is essentially zero for  $r \geq R$ .

The radial Schrodinger equation in this case is:

$$\phi''(k,r) + (k^2 - \frac{2m}{\hbar^2} V_0 f(r)) \phi(k,r) = 0 . \quad (\text{A.2})$$

It can be shown that in the asymptotic region  $r \geq R$ , the logarithmic derivative of the wavefunction  $L(k,r)$  is related to the scattering length  $a$  at zero energy by:

$$a = R - \frac{1}{L(0,R)} . \quad (\text{A.3})$$

The depth  $V_0$  which correctly produces the scattering length is the root of the equation:

$$G(V_0) \equiv a - R + \frac{1}{L(0,R)} = 0 . \quad (\text{A.4})$$

$G(V_0)$  can now be expanded in a Taylor series about some initial value of the strength  $V_I$ , such that  $V_0 = V_I + \Delta V$ , with the result:

$$\Delta V = - \frac{G(V_I)}{\frac{\partial G(V_I)}{\partial V_I}} \quad (A.5)$$

The partial derivative of  $G$  can be expressed as a function of the wavefunction logarithmic derivative using (A.4). That is:

$$\begin{aligned} \frac{\partial G(V_I)}{\partial V_I} &= - \frac{1}{L^2(0,R)} \frac{\partial L(0,R)}{\partial V_I} \\ &= - \frac{1}{(\phi'(0,R))^2} \int_0^R (\phi(0,r) \frac{\partial \phi''(0,r)}{\partial V_I} - \phi''(0,r) \frac{\partial \phi(0,r)}{\partial V_I}) dr. \quad (A.6) \end{aligned}$$

The integrand is determined directly from the radial equation (A.2) with  $k = 0$ .

$$\phi(0,r) \frac{\partial \phi''(0,r)}{\partial V_I} = \phi(0,r) \frac{2m}{\hbar^2} f(r) (\phi(0,r) + V_I \frac{\partial \phi(0,r)}{\partial V_I}) \quad (A.7)$$

and

$$\phi''(0,r) \frac{\partial \phi(0,r)}{\partial V_I} = \phi(0,r) \frac{2m}{\hbar^2} f(r) V_I \frac{\partial \phi(0,r)}{\partial V_I} \quad (A.8)$$

Subtracting (A.8) from (A.7) and substituting the result into (A.6) gives:

$$\frac{\partial G(V_I)}{\partial V_I} = - \frac{2m}{\hbar^2} \frac{1}{(\phi'(0,r))^2} \int_0^R \phi^2(0,r) f(r) dr \quad (A.9)$$



Using (A.4) and (A.9), the final expression for the correction to the potential depth  $\Delta V$  becomes:

$$\Delta V = \left( a - R + \frac{\phi(0,R)}{\phi'(0,R)} \right) \frac{\hbar^2}{2m} (\phi'(0,R))^2 / \int_0^R \phi^2(0,r) f(r) dr \quad (\text{A.10})$$

This final expression establishes the iterative scheme. For an initial guess of the strength  $V_I$  the radial equation is solved at zero energy for the wavefunction to the truncation point  $R$ . The correction to the strength  $\Delta V$  is determined from (A.10). This gives the new value of the depth  $V = V_I + \Delta V$ . This process can be repeated to any accuracy in the depth  $V_0$  and since this is a Newton-Raphson method quadratic convergence to the root  $V_0$  is assured.

## APPENDIX B

 $\Sigma$  ATOM COMPLEX ENERGY SHIFTS

The expression for the complex shifts (3.4.3) is derived from the radial Schrodinger equation describing the  $\Sigma$ -nucleus system.

$$\psi_{\Sigma}''(k,r) + \left( k^2 + \frac{2mc}{h} \frac{\alpha Z}{r} - \frac{\ell(\ell+1)}{r^2} - \frac{2m}{h} V_{\Sigma}(r) \right) \psi_{\Sigma}(k,r) = 0 \quad (B.1)$$

The regular and irregular solutions of (B.1) are denoted as  $\phi(k,r)$  and  $f(k,r)$  respectively, with  $\phi_c(k,r)$  and  $f_c(k,r)$  the corresponding solutions for the pure Coulomb case ( $V_{\Sigma} \equiv 0$ ).

It is assumed that the strong interaction  $V_{\Sigma}$  is short-ranged so that for some  $R$ ,  $V_{\Sigma}(r \geq R) = 0$ . The Jost function is defined as the Wronskian

$$\begin{aligned} L(k) &\equiv W[f(k,r), \phi(k,r)] , \\ &= W[f_c(k,r), \phi(k,r)] \quad r \geq R , \end{aligned} \quad (B.2)$$

since  $f_c(k,r)$  for  $r \geq R$  and  $V_{\Sigma} = 0$ .

The binding energy of the  $\Sigma^-$  corresponds to a zero of the Jost function<sup>(21)</sup>. From the definition of the Jost function, an equivalent condition is

$$G(k) \equiv \frac{\phi'(k,R)}{\phi(k,R)} - \frac{f_c'(k,R)}{f_c(k,R)} = 0 \quad (B.3)$$

Applying the Newton-Raphson method to (B.3),  $G(k)$  can be expanded in a Taylor series about some initial value of  $k$  such that  $k = k + \Delta k$ . That is:

$$\Delta k = - G(k) / \frac{\partial G(k)}{\partial k} . \quad (B.4)$$

The partial derivative of  $G$  can be determined directly from the definition (B.3) as:

$$\frac{\partial G(k)}{\partial k} = \frac{W[\phi(k,R), \dot{\phi}(k,R)]}{\phi^2(k,R)} - \frac{W[f_c(k,R), \dot{f}_c(k,R)]}{f_c^2(k,R)} , \quad (B.5)$$

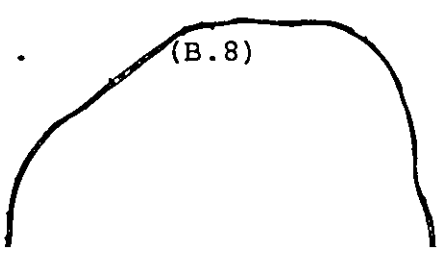
where the dot denotes differentiation with respect to  $k$ . The differentiated functions in (B.5) can be eliminated by returning to the radial equation (B.1). Differentiating the equation for  $\phi(k,r)$  with respect to  $k$  gives:

$$\frac{\partial \phi''(k,r)}{\partial k} + [k^2 + \frac{2mc}{\hbar} \frac{\alpha Z}{r} - \frac{l(l+1)}{r^2} - \frac{2m}{\hbar^2} V_\Sigma(r)] \frac{\partial \phi(k,r)}{\partial k} = -2k\phi(k,r) . \quad (B.6)$$

Multiplying (B.1) and (B.6) by  $\partial \phi(k,r) / \partial k$  and  $\phi(k,r)$  respectively, and subtracting, gives:

$$\frac{d}{dr} W[\phi(k,r), \dot{\phi}(k,r)] = -2k\phi^2(k,r) . \quad (B.7)$$

Similarly for the irregular solution  $f_c(k,r)$ :

$$\frac{d}{dr} W[f_c(k,r), \dot{f}_c(k,r)] = -2kf_c^2(k,r) . \quad (B.8)$$


Integrating (B.7) and (B.8) from  $0 \rightarrow R$  and  $R \rightarrow \infty$  respectively, and inserting into (B.5) gives  $\partial G(k)/\partial k$  as:

$$\frac{\partial G(k)}{\partial k} = -2k \left[ \int_0^R \left( \frac{\phi(k,r)}{\phi(k,R)} \right)^2 dr + \int_R^\infty \left( \frac{f_c(k,r)}{f_c(k,R)} \right)^2 dr \right] \quad (B.9)$$

Since  $R$  is assumed to be small, the second integral is large compared with the first, so to a good approximation  $R$  can be replaced by  $0$  in the integrals. The expression (B.4) for  $\Delta k$  then becomes:

$$\Delta k = \frac{f_c(k,R)}{\phi(k,R)} W[f_c(k,r), \phi(k,R)] / (-2k \int_0^\infty f_c^2(k,r) dr) \quad (B.10)$$

It is known that the complex shifts are small compared with the unperturbed Coulomb energies. If the initial value of  $k$  used corresponds to the unperturbed value  $k_0$  it has been shown that only one iteration is required to achieve an accuracy of 4% or better<sup>(15)</sup>.

For  $k = k_0$ , the function  $f_c(k_0, r)$  is proportional to the regular solution  $\phi_c(k_0, r)$ <sup>(21)</sup> and the expression for the energy shift  $\delta E$  is then:

$$\delta E = -\frac{\hbar^2}{2m} \cdot \left[ \frac{\phi'(k_0, R)}{\phi(k_0, R)} \frac{\phi_c'(k_0, R)}{\phi_c(k_0, R)} \right] / \int_0^\infty \left( \frac{\phi_c(k_0, r)}{\phi_c(k_0, R)} \right)^2 dr \quad (B.11)$$

In the  $\Sigma^-$  atoms the orbits of interest are the circular orbits. The analytic expression for these wavefunctions is well-known

(see for example, ref. 8) so substituting for  $\phi_c(k_0, r)$  and  $\phi_c'(k_0, r)$  in (B.11) produces a convenient form for the complex shift:

$$\delta E = -\frac{\hbar^2}{2m} \cdot e^{2ik_0 R} (-2ik_0 R)^{2\ell+3} \left( R \cdot \frac{\phi_c'(k_0, R)}{\phi_c(k_0, R)} - \ell(\ell+1) - ik_0 R \right) / R^2 \cdot \Gamma(2\ell+3).$$

(B.12)

This final expression is suited to numerical work in that the strong interaction dependence enters only through the logarithmic derivative of the perturbed  $\Sigma$  wavefunction.

## APPENDIX C

### POTENTIAL OPTIMIZATION PROGRAM

```

5      PROGRAM FATS0 (INPUT, OUTPUT, TAPES=INPUT, TAPES=OUTPUT)
.....
PURPOSE:
10     PROGRAM FATS0 OPTIMIZES THE SIGMA-NUCLEON POTENTIAL PARAMETERS,
        BY MINIMIZING THE CHI-SQUARE DEVIATION FROM THE COMBINED
        ATOMIC AND SCATTERING LENGTH DATA.

15     THE INITIAL VALUES OF THE POTENTIAL PARAMETERS IN THE ARRAY VARY
        ARE SENT TO THE SUBROUTINE NINFUN. NINFUN USES THE SUBROUTINE
        CHISQR TO CALCULATE THE CHI-SQUARE DEVIATION FROM THE EXPERIMENTAL
        ATOMIC LEVEL SHIFTS AND THE SCATTERING DATA. NINFUN VARIES THE
        POTENTIAL PARAMETERS TO MINIMIZE THE CHI-SQUARE. THE ATOMIC LEVEL
        SHIFTS ARE CALCULATED IN SUBROUTINE ATOM AND THE SCATTERING
        LENGTHS IN SUBROUTINE SCATL.

20     DESCRIPTION OF PARAMETERS:
        VARY - ARRAY CONTAINING THE POTENTIAL PARAMETERS.
                VARY(1) - SIGMA-N S=0 REAL POTENTIAL DEPTH.
                VARY(2) - SIGMA-N S=1 REAL POTENTIAL DEPTH.
                VARY(3), VARY(4) - SIGMA-P S=0 REAL AND IMAGINARY
                                POTENTIAL STRENGTHS.
                VARY(5), VARY(6) - SIGMA-P S=1 REAL AND IMAGINARY
                                POTENTIAL STRENGTHS.
                VARY(7) - INVERSE POTENTIAL RANGE.
        NDATA - TOTAL NUMBER OF DATA POINTS.
        NATOM - NUMBER OF ATOMS.
        HOENS - ARRAY OF HALF-DENSITY RADII OF ATOMS.
        SKIN  - ARRAY OF NUCLEAR SKIN THICKNESS PARAMETERS.
        ATNUF - ARRAY CONTAINING ATOMIC NUMBERS.
        ANUCLM - ARRAY OF NUCLEAR MASSES (MEV).
        PNUM  - ARRAY OF PROTON NUMBERS.
        ANGM  - ARRAY OF ATOMIC ORBITAL ANGULAR MOMENTUM QUANTUM
                NUMBERS FOR THE LOWER CIRCULAR ORBIT OF THE TRANSITIONS.
        SHIFT - ARRAY OF EXPERIMENTAL ENERGY SHIFTS (EVI). THE LOWER,
                THEN UPPER LEVEL VALUES ARE READ-IN FOR EACH ATOM
                CONSECUTIVELY.
        DSHIFT - EXPERIMENTAL UNCERTAINTIES IN THE LEVEL SHIFTS.
        GAMMA - ARRAY OF EXPERIMENTAL LEVEL WIDTHS (EVI).
        CGAMMA - EXPERIMENTAL UNCERTAINTIES IN THE LEVEL WIDTHS.
        NSCATL - NUMBER OF SCATTERING LENGTHS.
        RSL   - ARRAY OF EXPERIMENTAL SCATTERING LENGTHS. THESE
                ARE READ IN THE ORDER: SIGMA-N S=0,1; SIGMA-P S=0,1.
                THE REAL AND IMAGINARY COMPONENTS ARE READ
                ALTERNATELY. SIGMA-NEUTRON IMAGINARY COMPONENTS
                MUST BE SET EQUAL TO ZERO.
        ERRSL - ARRAY OF EXPERIMENTAL ERRORS IN SCATTERING LENGTHS.
        S,ZS  - ARRAYS CONTAINING CONSTANTS USED IN THE CALCULATION OF
                SCATTERING LENGTHS IN SUBROUTINE SCATL. THE VALUES
                GIVEN HERE ARE EXPLICITLY FOR USE WITH YUKAWA POTENTIALS.
        G,M   - GAUSS WEIGHTS AND COORDINATES.
        NOPS  - NUMBER OF GAUSS POINTS.
        INCEST - CONTROL PRINTING.
                INCEST = 1 ON THE FIRST ENTRY TO CHISQR. THIS CAUSES
                PRINTING OF THE CALCULATED ATOMIC SHIFTS AND SCATTERING
                LENGTHS RESULTING FROM THE INITIAL VALUES OF THE
                PARAMETERS IN VARY. INCEST IS AGAIN SET = 1 AT THE
                END OF THE OPTIMIZATION AND THE CALCULATED VALUES OF
                THE SHIFTS AND SCATTERING LENGTHS ARE PRINTED ALONG
                WITH THE CHI-SQUARE AND REDUCED CHI-SQUARE.
    
```

```

65 DIMENSION VARY(50),E(50)
   DIMENSION WORK(500)
   DIMENSION SL(50)
   COMPLEX VNUCR
   COMPLEX VO
   EXTERNAL CHISQR
70 EXTERNAL CZRIVN,CONV,GAIN
   COMMON/C1/REON,ALPHA,Z,SORKO,AM,VNUCR
   COMMON/C2/AD,CO,NO
   COMMON/C3/BETA
75 COMMON/C4/MBAR,C,MOARC,SIGMA,REDNSN,TWOPI,FOURPI
   COMMON/C5/G(4),M(4),NOPS
   COMMON/C6/A(4),M(3),H(3)
   COMMON/C7/S(4),Z(4)
80 COMMON/C8/NATOM,NATOM2,PNUM(50),ATNUM(50),HDENS(50),SKIN(50),
   1 ANUCLM(50),ANGM(50)
   COMMON/C9/NPARAM
   COMMON/C10/SHIFT(50),CSHIFT(50),GAMMA(50),CGAMMA(50)
   COMMON/C11/NSCATL,NSL(50),ERRSL(50)
   COMMON/C12/INCEST
90 COMMON/C13/VO
   DATA S/1.0799,0.4504,14.324,27.4745/
   DATA ZS/0.4671,11.852,22.041,302.4012/
   READ(5,41) (A(I),I=1,4)
95 READ(5,43) (N(I),I=1,3)
   JO = 1E2,4
   H(I=1)=1-(I)-A(I-1)/FLOAT(N(I-1))
   9 CONTINUE
   READ(5,11) INDATA
100 READ(5,11) INATOR
   FORMAT(11,1)
11 READ(5,25) (PNUM(I),ATNUM(I),HDENS(I),SKIN(I),ANUCLM(I),ANGM(I),
   1 I=1,NATOM)
   11 FORMAT(7F10.5)
   READ(5,11) NPARAM
105 FORMAT(6F10.5)
   READ(5,23) (VARY(I),I=1,NPARAM)
   READ(5,23) (E(I),I=1,NPARAM)
   READ(5,27) ICON,IPRINT,MAXIT,ESCALE
17 FORMAT(11IC,F10.5)
   NATOM2=2*NATOM
19 READ(5,21) (SHIFT(I),CSHIFT(I),GAMMA(I),CGAMMA(I),I=1,NATOM2)
   19 FORMAT(4F10.5)
   READ(5,21) (NSCATL
110 READ(5,21) (SL(I),ERRSL(I),I=1,NSCATL)
   READ(5,21) NOPS
   21 FORMAT(18)
   READ(5,23) (G(I),M(I),I=1,NOPS)
   23 FORMAT(6F10.5)
   WORK=NPARAM*(NPARAM+3)
115 NBAR=0.50E11E-22
   C=2.00E11E-23
   H=10.00E-20
   FOURPI=4.*PI
   SIGMA=1.7E-35
120 PNUMEAN=1.0E-35
   REDNSN=2.0*(PNUMEAN*SIGMA)/(PNUMEAN+SIGMA)/(444AC**2)
   WRITE(6,25)
   INCEST=1
125 CALL MINFUN(VARY,E,NPARAM,X2,ESCALE,IPRINT,ICON,MAXIT,WORK,
   1 WORK,CHISQR)
   1 WRITE(6,25)
   25 FORMAT(11)
   INCEST=1
130 CALL CHISQR(NPARAM,VARY,X2)
   REDX=X2/FLOAT(INDATA-NPARAM)
   WRITE(6,27) REDX2
   27 FORMAT(17X,"TOTAL REDUCED X2=",12X,F10.5/)
   WRITE(6,29) (PARV(I),I=1,NPARAM)
135 FORMAT(17X,"CONVERGED PARAMETERS ARE",F10.4,/,26X,F15.3,/,25X,
   1 F15.8,"J",/,26X,F15.8,"J",/,25X,F15.8)
   WRITE(6,25)
   WRITE(6,31)
140 FORMAT(7,23X,"EXPERIMENTAL DATA",/24X,"ATOMIC",/)
   WRITE(6,31)
   31 FORMAT(17X,"EPSILON",17X,"GAMMA",/)
   WRITE(6,35) (SHIFT(I),CSHIFT(I),GAMMA(I),CGAMMA(I),I=1,NATOM2)
145 FORMAT(7X,F8.3,"",F8.2,/,26X,F8.2,"",F8.2)
   WRITE(6,37)
   37 FORMAT(7,23X,"SCATTERING",/)
   WRITE(6,39) (SL(I),ERRSL(I),I=1,NSCATL)
150 FORMAT(7X,F10.3,"",F8.3,/,26X,F8.3,"",F8.3,/,26X,F8.3)
   41 FORMAT(11IC)
   43 FORMAT(11IC)
   STOP
   END

```

```

1 SUBROUTINE MINFUN(X,E,U,F,ESCALE,IPRINT,ICON,MAXIT,NWORK,CALCFX)
.....

```

## PURPOSE:

```

5 MINFUN FINDS THE MINIMUM VALUE OF A FUNCTION BY ITERATIVE
  VARIATION OF THE FUNCTION PARAMETERS.
  THE PARAMETERS NEED NOT BE INDEPENDENT.
  THE METHOD IS AN UPDATED VERSION OF A ROUTINE BY N. POWELL
  PUBLISHED IN THE COMPUTER JOURNAL(1964).

```

## DESCRIPTION OF PARAMETERS:

```

10 N - NUMBER OF PARAMETERS IN OPTIMIZATION.
  X - ARRAY OF PARAMETERS. X(1) MUST BE SET TO AN
  APPROXIMATION OF THE I-TM PARAMETER.
15 E - ARRAY CONTAINING THE ABSOLUTE ACCURACIES TO
  WHICH THE PARAMETERS ARE REQUIRED.
  - THE MAGNITUDES OF THE E(I) ARE ASSUMED TO BE
  ROUGHLY THE SAME AS THE N(I).
20 F - FUNCTION VALUE RETURNED BY CALCFX.
  M - AUXILIARY WORK ARRAY OF DIMENSION NWORK.
  - NWORK MUST BE SPECIFIED TO BE AT LEAST N*(N+3)
  IN CALLING PROGRAM.
25 ICON - CONTROLS THE ULTIMATE CONVERGENCE CRITERIA.
  *1 CONVERGENCE WILL BE ASSUMED WHEN AN
  ITERATION CHANGES EACH VARIABLE BY LESS
  THAN 0.3 PERCENT OF THE ACQUIRED ACCURACY.
  *2 A POINT SUCH AS FOR ICON=1 IS FOUND AND
  THEN DISPLACED BY TEN TIMES THE REQUIRED
  ACCURACY IN EACH PARAMETER. MINIMIZATION
  IS CONTINUED FROM THE NEW POINT UNTIL
  A 10 PERCENT ACCURACY IS AGAIN ACHIEVED.
  THE TWO ESTIMATES OF THE MINIMA ARE COMPARED.
30 IPRINT - CONTROLS PRINTING.
  *1 THERE WILL BE NO PRINTING.
  *2 THE VARIABLES AND FUNCTION WILL BE PRINTED
  AFTER EVERY SEARCH ALONG A LINE (APPROXIMATELY
  EVERY OTHER FUNCTION VALUE).
  *3 THE VARIABLES AND FUNCTION VALUE WILL BE
  PRINTED AFTER EVERY ITERATION (N+1 SEARCHES
  ALONG A LINE).
35 MAXIT - MAXIMUM NUMBER OF ITERATIONS.
  ESCALE - LIMITS THE MAXIMUM CHANGES IN THE PARAMETERS.
  - X(I) WILL NOT BE CHANGED BY MORE THAN ESCALE*E(I)
  AT A SINGLE STEP.
40
45

```

## FUNCTIONS AND SUBROUTINES REQUIRED:

```

50 CALCFX(X,F)
  EXTERNAL SUBROUTINE TO CALCULATE THE FUNCTION VALUE
  FOR A GIVEN SET OF THE PARAMETERS X(I).

```

```

  DIMENSION NWORK(1,XIN),E(1)

```

```

55 DIMAG=1./ESCALE
  SCERR=.001/ESCALE
  JJ=N*N
  JJJ=JJ*N
  KKK=1
  NFOC=1
  IND=1
  INN=1
  DO 1 I=1,N
  DO 2 J=1,N
60 W(I)=C.
  IF(I=J) W(I)=X(I)
  W(I)=X(I)+STE(1)
  W(I)=X(I)+ESCALE
  KKK=1
  2 CONTINUE
  1 CONTINUE
  IT=1
  ISG=1
  CALL CALCFX(X,F)
  FKEEP=100.(2.*F)
75 ITONE=1
  F=1
  SUM=0
  IPR=JJ
  DO 3 I=1,N
  XP=X(I)
  X(I)=W(I)
  3 CONTINUE

```



```

IDIRN=PI
ILINE=1
85 7 OMAX=I(LINE)
   DACC=OMAX*SSER
   OMAG=AMIN(IOMAG,.1*OMAX)
   OMAG=AMAX(IOMAG,20.*DACC)
   OMAX=13.*OMAG
90 *F(TORE=2)70,71
7C OL=3.
   O=OMAG
   FPR=V*F
   IS=5
95 FA=F
   OA=CL
6 JD=D-OL
   OL=D
58 K=IOIRN
   DO 9 I=1,N
   X(I)=X(I)+OD*W(K)
   K=K+1
9 CONTINUE
   F(TORE)=F
105 CALL CALCFX(N,X,F)
   FCC=FCC+1
   GOTD (1,2,11,12,13,14,96),IS
14 IF (F-F3) 15,16,24
16 IF (ABS(OI-OMAX))17,17,18
17 DC=D
   GOTO 4
1A PRINT 1)
19 FORMAT(5X,4SMINIMUM MAXIMUM CHANGE DOES NOT ALTER FUNCTION)
   GOTO 20
115 15 FB=F
   DB=D
   GOTD 21
24 FA=FA
   DB=DA
120 FA=F
   DA=D
21 IF (IGGRAD)1133,33,23
23 O=OB+DB-CA
   IS=1
   GOTO 3
125 43 O=.5*(OA+OB-(FA-F3)/(CA-DB))
   IS=4
   IF ((OA-OI)*(O-DB))25,3,8
25 IS=1
130 IF (ABS(O-DB)-OMAX)18,1,26
26 O=OB+SIGN(OO-AX,OO-DA)
   IS=1
   OI=OX+COMAX*COMAX
   OJNAG=COMAG*COMAG
   IF (COMAX-CMAA)3,3,17
135 27 COMAX*COMAX
   GOTO 4
14 13 IF (F-F4)19,23,23
140 48 FC=F3
   DC=D
24 FA=F
   DB=D
   GOTO 10
12 IF (F-F2)28,23,31
1-5 31 FA=F
   OA=D
   GO TO 33
15 IF (F-F3)32,10,10
190 32 FA=F3
   OA=OB
   GOTD 29
71 OL=1.
   OJMAX=5.
   FA=FP
255 OA=-1.
   F3=FHOLO
   OJ=D.
   O=1.
16 FC=F
   DC=D
260 30 A=(OB-CC)*(FA-FC)
   B=(CC-CA)*(FN-FC)
   IF ((A+B)*(CA-CC))33,33,34

```

```

165 33 FA=FB
    DA=OB
    FR=FC
    DI=OC
    GOTO 25
170 34 O=.5*(A*(OB+DC)+B*(JA+DC))/(A+B)
    DI=DO
    FI=FO
    IF (FB-FC)4,4,4,4,3
    3 DI=DC
    FI=FC
175 44 IF (ITONE-2)86,86,85
    45 ITONE=2
    GOTO 5
180 86 IF (ABS(D-DI)-DACC)41,41,93
    93 IF (ABS(D-DI)-.01*ABS(DI))41,41,999
    999 IF (ABS(F-FSTORE)-.01*ABS(FI))41,42,45
    45 IF ((DA-DC)*(OC-DI))47,46,46
    46 FA=FR
    DA=OB
    FR=FC
    DI=OC
185 47 GOTO 25
    IS=2
    IF ((DA-DI)*(OC-DC))48,8,8
    44 IS=3
    GOTO 8
190 41 F=FI
    O=DI-OL
    DO=50*(OC-OB)*(OC-DA)*(OC-OB)/(A+B)
    DO=49 I=1,N
195 XI(I)=X(I)+J*(OIRN)
    XI(I)=X(I)+J*(OIRN)
    OIRN=OIRN+1
    49 CONTINUE
    W(I,LINE)=W(I,LINE)/DO
    ILINE=ILINE+1
    50 IF (PRINT-1)51,50,51
200 50 PRINT 52,ITERC,AFCC,F,(X(I),I=1,N)
    52 FORMAT(7X,6H ITERATION,15,115,16H FUNCTION VALUES,
    1 1X,3HF,4E21,14/4E24,14J)
205 1 IF (PRINT-1)51,51,53
    51 IF (ITONE-1)55,55,38
    55 IF (F-PPREV-F-SUM)94,95,95
    95 SUM=F-PPREV-F
    JIL=ILINE
210 94 IF (J-JJ)17,7,14
    8 IF (IND-1)92,92,72
    92 FMOLD=F
    IS=5
    IXP=J
215 DO 54 I=1,N
    IXP=IXP+1
    W(IXP)=X(I)-W(IXP)
    53 CONTINUE
    OJ=1
220 GOTO 54
    78 IF (IND-1)12,12,47
    12 IF (F-PPREV-F)37,37,51
    94 J=2*(F-PPREV-F-2*FMOLD)/(F-PPREV-F)
    92 IF (J*(F-PPREV-F-SUM)**2-SUM)17,37,37
225 87 J=JIL*N+1
    IF (J-JJ)60,60,61
    60 DO 62 I=J,JJ
    K=I-N
230 W(K)=W(I)
    52 CONTINUE
    DO 37 I=JIL,N
    W(I)=W(I)
    17 CONTINUE
235 61 I=I+1
    OIRN=OIRN
    IY=JJ
    AA=53
    DO 65 I=1,N
    IXP=IXP+1
    W(K)=W(IXP)
    66 IF (ABS(W(K)/E(I))
240 66 W(K)=1
    65 CONTINUE
245 65 CONTINUE

```

```

DOMAG=1.
W(1)=SCALE/AAA
ILINE=N
GOTO 7
250 37 IXP=JJ
    AAA=0.
    F=FNOLD
    DO 99 I=1,N
    IXP=IXP+1
255 71 W(I)=X(I)-W(IXP)
    IF (AAA*ABS(E(I))-ABS(W(IXP))) 98,99,99
94 91 AAA=ABS(W(IXP)/E(I))
99 CONTINUE
GOTO 72
260 98 AAA=AAA*(1+.01)
    IF (IND-1) 72,72,106
72 IF (IND-1) 72,72,106
53 IF (IND-1) 109,109,83
104 IF (AAA-1) 109,109,76
265 99 IF (ICON-1) 20,20,126
110 IND=2
    IF (INN-1) 100,100,101
100 INN=2
    <<JJJ
270 DO 102 I=1,N
    K=K+1
    W(K)=X(K)
    X(I)=X(I)+10.*E(I)
102 CONTINUE
275 FKEEP=F
    CALL CALCFX(N,X,F)
    NFCC=NFCC+1
    DOMAG=0.
    GOTO 108
280 76 IF (F-FKEEP) 76,76
78 PRINT 50
80 FORMAT(5X,34MINIFUN ACCURACY LIMITED BY ERRORS IN F)
    GOTO 20
285 88 IND=1
35 DOMAG=.1*SQRT(F-F)
    ISGRAD=1
108 ITERC=ITERC+1
    IF (ITERC-PA) 115,5,81
293 81 PRINT 82,PA
82 FORMAT(10,31, ITERATIONS COMPLETED BY MINIFUN)
    IF (F-FKEEP) 100,20,110
110 F=FKEEP
    DO 111 I=1,N
    JJJ=JJJ+1
    X(I)=W(JJJ)
295 111 CONTINUE
    GOTO 20
101 JIL=1
    F=FKEEP
300 IF (F-FKEEP) 105,76,104
104 JIL=2
    F=F
305 IXP=JJ
    DO 113 I=1,N
    IXP=IXP+1
    K=IXP+K
    IF (JIL-1) 114,114,115
310 114 W(IXP)=W(K)
    GOTO 113
115 W(IXP)=X(I)
    X(I)=W(K)
113 CONTINUE
    JIL=2
315 GOTO 92
106 IF (AAA-0.1) 20,20,107
20 RETURN
107 END
320 GOTO 35
    END

```

```

1      SUBROUTINE CHISQR(NPARAM,VARY,CHSOR)
2      *****
3
4      PURPOSE:
5      CHISQR CALCULATES THE CHI-SQUARE DEVIATION OF THE COMBINED
6      ATOMIC AND SCATTERING LENGTH DATA FOR A GIVEN SET OF THE
7      POTENTIAL PARAMETERS.
8
9      DESCRIPTION OF PARAMETERS:
10     VARY - ARRAY OF POTENTIAL PARAMETERS.
11     CHSOR - TOTAL CHISQUARE RETURNED TO MINFUN.
12     NPARAM - NUMBER OF VARIATIONAL PARAMETERS.
13     ATOMXZ - ARRAY CONTAINING THE ATOMIC SHIFT AND WIDTH DATA
14             CALCULATED BY ATOM.
15     XZATCH - CHI-SQUARE DEVIATION OF THE CALCULATED ATOMIC
16             SHIFT DATA.
17     SLXZ - ARRAY OF THE SCATTERING LENGTHS CALCULATED BY SCATL.
18     XZSL - CHI-SQUARE DEVIATION OF THE CALCULATED SCATTERING
19             LENGTHS.
20     SHIFT - ARRAY CONTAINING THE EXPERIMENTAL ATOMIC LEVEL
21             SHIFTS OF DIMENSION NATOM2.
22     DSHIFT - ARRAY OF THE EXPERIMENTAL ERRORS IN THE SHIFTS.
23     GAMMA - ARRAY CONTAINING THE EXPERIMENTAL ATOMIC LEVEL
24             WIDTHS.
25     OGAMMA - ARRAY OF THE EXPERIMENTAL ERRORS IN THE WIDTHS.
26     RSL - ARRAY OF THE EXPERIMENTAL SCATTERING LENGTHS OF
27           DIMENSION NSCATL.
28     ERRSL - ARRAY OF EXPERIMENTAL ERRORS IN SCATTERING LENGTHS.
29     INCEST - DETERMINES PRINTING.
30             *1 THE CHI-SQUARES WILL BE PRINTED.
31             *0 NO PRINTING.
32
33     FUNCTIONS AND SUBROUTINES REQUIRED:
34     ATOM(VARY,ATOMXZ)
35     SUBROUTINE TO CALCULATE THE ATOMIC SHIFTS AND WIDTHS.
36     SCATL(VARY,SLXZ)
37     SUBROUTINE TO CALCULATE THE SCATTERING LENGTHS RESULTING
38     FROM THE POTENTIAL PARAMETERS IN VARY.
39
40     DIMENSION ATOMXZ(50),SLXZ(50),VARY(50)
41     COMMON/CA/NATOM,NATOM2,PNUM(50),ATNUM(50),MDENS(50),SKIN(50),
42     1 ANUCLM(50),ANGM(50)
43     COMMON/C10/SHIFT(50),DSHIFT(50),GAMMA(50),OGAMMA(50)
44     COMMON/C11/NSCATL,RSL(50),ERRSL(50)
45     COMMON/C12/INCEST
46
47     XZSL=0.
48     XZATOM=0.
49     CALL SCATL(VARY,SLXZ)
50     DO 3 I=1,NSCATL
51     XZSL=XZSL+((SLXZ(I)-RSL(I))/ERRSL(I))**2
52     3 CONTINUE
53     CHSOR=XZSL*XZATOM
54     *IF INCEST.EQ.1,17,11
55     7 WRITE(6,*)XZSL,XZATOM,CHSOR
56     9 FORMAT(1X,'SL XZ, ATOMIC XZ AND TOTAL XZ',2F10.5,5X,F10.5)
57     11 INCEST=INCEST*1
58
59     RETURN
60     END

```

```

1      SUBROUTINE ATOM(VARY,CSHIFT)
2      *****
3      PURPOSE:
4      ATOM CALCULATES THE ENERGY LEVEL SHIFTS AND WIDTHS IN
5      THE CIRCULAR ATOMIC ORBITALS FOR BOTH THE UPPER AND LOWER
6      LEVELS OF THE TRANSITION. THESE ARE CALCULATED FOR ALL
7      ATOMS SPECIFIED.
8      THE METHOD USED IS DUE TO A. DELOFF, PHYS. REV., C13, 2 (1976).
9
10     DESCRIPTION OF PARAMETERS:
11     EO      = UNPERTURBED COULOMB ENERGY OF THE ATOMIC LEVEL.
12     AM      = ANGULAR MOMENTUM QUANTUM NUMBER FOR THE ORBITAL.
13     AO      = NUCLEAR SKIN THICKNESS.
14     CO      = NUCLEAR HALF-DENSITY RADIUS.
15     RO      = DENSITY NORMALIZATION CONSTANT.
16     VARY    = ARRAY OF POTENTIAL PARAMETERS.
17     VONS    = SIGMA-NEUTRON SPIN-SINGLET POTENTIAL DEPTH.
18     VONT    = SIGMA-NEUTRON SPIN-TRIPLET POTENTIAL DEPTH.
19     VOPS    = SIGMA-PROTON SPIN-SINGLET POTENTIAL DEPTH.
20     VOPT    = SIGMA-PROTON SPIN-TRIPLET POTENTIAL DEPTH.
21     VON     = SPIN-AVERAGED SIGMA-NUCLEON POTENTIAL DEPTH.
22     VOP     = SPIN-AVERAGED SIGMA-PROTON POTENTIAL DEPTH.
23     VNR     = VALUE OF POTENTIAL DENSITY FOLDING INTEGRAL
24             AT THE POINT R.
25     VNUCR   = TOTAL SIGMA-NUCLEUS STRONG INTERACTION AT R.
26     VO      = TOTAL SIGMA-NUCLEUS POTENTIAL DEPTH.
27     ZN(1)   = WAVEFUNCTION VALUE.
28     ZN(2)   = FIRST DERIVATIVE OF THE WAVEFUNCTION.
29     DELTAE  = COMPLEX ENERGY LEVEL SHIFT (EV).
30     CSHIFT  = ARRAY CONTAINING THE ATOMIC COMPLEX SHIFTS
31             RETURNED TO CMISSOR.
32     INCEST  = CONTROLS PRINTING.
33             *1 THE NUCLEAR CHARGE Z, ANGULAR MOMENTUM
34             QUANTUM NUMBER L OF THE ORBITAL, AND THE
35             RESULTING COMPLEX SHIFT WILL BE PRINTED.
36             *2 NO PRINTING.
37
38     COMPLEX ZN(2), ZNPRIM(2)
39     COMPLEX VO, VON, VOP, VONS, VONT, VOPS, VOPT
40     COMPLEX VNUCR, DELTAE
41     DIMENSION VARY(50)
42     DIMENSION CSHIFT(50)
43     COMMON/C1/REOM,ALPHA,Z,SORKO,AM,VNUCR
44     COMMON/C2/CO,RO
45     COMMON/C3/BETA
46     COMMON/C4/HHAR,C,HSARC,SIGMAR,REOMSN,THOPI,FOURPI
47     COMMON/C5/A(4),N(1),H(1)
48     COMMON/C6/NATOM,NATOM2,PNUM(50),ATNUM(50),HDENS(50),SKIN(50),
49             ANUCLM(50),ANGM(50)
50     COMMON/C12/INCEST
51     EXTERNAL DERIVN,CONV
52
53     M=1
54     NE=2
55     VONS=CMPLX(VARY(1),0.)
56     VONT=CMPLX(VARY(2),0.)
57
58     VOPS=CMPLX(VARY(3),VARY(4))
59     VOPT=CMPLX(VARY(5),VARY(6))
60     BETA=VARY(7)
61     VON=(VONS+3.*VONT)/4.
62     VOP=(VOPS+3.*VOPT)/4.
63     IF(INCEST.EQ.1)1,3
64
65     *1
66     WRITE(6,7)
67     DO 15 L=1,NATOM
68     AO=SKIN(L)
69     CO=HDENS(L)
70     RO=(3./((FCURPI*CO**3))/(1.+(4.*ATAN(1.)*AO/CO)**2)
71     Z=PNUM(L)
72     ATMASS=ANUCLM(L)*931.481
73     AMEAN=ATMASS*SIGMAR/(ATMASS+SIGMAR)
74     ALPHA=2.*AMEAN/(HHAR*C*1.37*0.36)
75     REOM=2.*AMEAN/(HHAR*C**2)
76     AM=ANGM(L)
77     XP=Z
78     WN=ATNUM(L)-PNUM(L)
79     VO=WN*VON+VOP
80     DO 13 J=1,2
81     EO=-6.5*AMEAN*((Z/137.036)**2)/((AM+1.1)**2)
82     RKO=AMEAN/(HHAR*C)*(Z/137.036)/(AM+1.1)
83     SORKO=RKO**2
84     R=0.
85     ZN(1)=(0.,0.)
86     ZN(2)=(0.,0.)
87     VNUCR=(0.,0.)
88     DO 7 K=1,3
89     NN=N(K)
90     DO 5 I=1,NN
91     CALL GILSIP(P,H(K),NE,ZN,ZNPRIM,DERIVN)
92     CALL GAINT(C,16.,R,CONV,VNR)
93     VNUCR=VO+VNR
94     CONTINUE
95     *2
96     DELTAE=XP-2.*RKO*A(4)*((12.*RKO*A(4))**2*(AM+3.11)*
97     A(4)*ZN(2)/ZN(1)-(AM+1.1)*A(4)*RKO*1.506/REOM*(A(4)**2.1)*
98     B FACTOR(2,AM+2.1)
99     IF(INCEST.EQ.1)1,11
100    *1
101    WRITE(6,10)Z,AM,REAL(-DELTAE),%IMAG(-DELTAE)
102    CSHIFT(M)=REAL(-DELTAE)
103    CSHIFT(M+1)=IMAG(-DELTAE)
104    MEM=2
105    AM=AM+1.
106    CONTINUE
107    CONTINUE
108    CONTINUE
109    FJPHAT(/94,"Z",10X,"L",7X,"EPSILON",10X,"GAMMA")
110    FORMAT(/1X,2F10.0,2F15.3)
111    RETURN
112    END

```

```

1          SUBROUTINE GILSTP(X,N,H,Y,Z,DERIV)
          .....
5          PURPOSE:
          GILSTP SOLVES N, COUPLED, FIRST-ORDER DIFFERENTIAL
          EQUATIONS BY THE GILL MODIFIED RUNGE-KUTTA METHOD.
10         DESCRIPTION OF PARAMETERS:
          X - INITIAL VALUE OF INDEPENDENT PARAMETER.
          H - STEP-SIZE FOR INCREMENTING X.
          N - NUMBER OF COUPLED EQUATIONS (MAXIMUM OF 12).
          Y - ARRAY OF INITIAL VALUES OF FUNCTIONS.
          Z - ARRAY OF FUNCTION DERIVATIVES CALCULATED BY DERIV
15         FUNCTIONS AND SUBROUTINES REQUIRED:
          DERIV(X,N,Y,Z)
          SUBROUTINE TO CALCULATE FUNCTION DERIVATIVES.
20         COMPLEX Y(12),Z(12),O(12)
          CALL DERIV(X,N,Y,Z)
          DO 3 I=1,N
          Y(I)=Y(I)+H*Z(I)/2.
25         3 O(I)=Z(I),
          X=X+H/2.
          CALL DERIV(X,N,Y,Z)
          DO 5 I=1,N
          Y(I)=Y(I)+H*.2928932148 * (Z(I)-O(I))
30         5 O(I)=.5957664376 * Z(I) + 0.12132034356 * O(I)
          CALL DERIV(X,N,Y,Z)
          DO 7 I=1,N
          Y(I)=Y(I)+H*1.7371067412 * (Z(I)-O(I))
35         7 O(I)=.3284271248 * (Z(I)-O(I))-1.4142135624 * O(I)
          X=X+H/2.
          CALL DERIV(X,N,Y,Z)
          DO 9 I=1,N
          Y(I)=Y(I)+H*(Z(I)-O(I))/6.
          RETURN
          END

```

```

1          SUBROUTINE DERIVN(R,N,ZN,ZPRIME)
          .....
5          PURPOSE:
          DERIVN IS USED IN CONJUNCTION WITH GILSTP AND DEFINES
          THE FUNCTION DERIVATIVES APPEARING IN THE SCHRODINGER
          EQUATION FOR THE ATOMIC PROBLEM.
10         DESCRIPTION OF PARAMETERS:
          ZN(1) - WAVEFUNCTION VALUE.
          ZN(2) - FIRST DERIVATIVE OF WAVEFUNCTION.
          ZPRIME(1) - FIRST DERIVATIVE OF WAVEFUNCTION (SAME AS ZN(2)).
          ZPRIME(2) - SECOND DERIVATIVE OF WAVEFUNCTION.
15         Z - NUCLEAR CHARGE.
          AM - ANGULAR MOMENTUM QUANTUM NUMBER L.
          REDM - TWICE THE REDUCED MASS OF THE SIGMA-NUCLEUS
          SYSTEM DIVIDED BY HBAR**2.
20         VNUCR - COMPLEX SIGMA-NUCLEUS POTENTIAL AT DISTANCE R
          FROM NUCLEAR CENTRE.
          ALPHA - FINE STRUCTURE CONSTANT.
          SORKO - UNPERTURBED COULOMB ENERGY OF ATOMIC ORBITAL.
25         COMPLEX ZN(2),ZPRIME(2)
          COMPLEX VNUCR
          COMMON/C1/REDM,ALPHA,Z,SORKO,AM,VNUCR
          ZPRIME(1)=ZN(2)
          IF (Z)5,5,3
30         3 ZPRIME(2)=(REDM*VNUCR-ALPHA*Z/R+AM*(AM+1.)/(R**2)+SORKO)*ZN(1)
          RETURN
          ZPRIME(2)=(0.,0.)
5          RETURN
          END
35

```

```

1  SUBROUTINE GAINT(A,R,F,SUM)
2  .....
3  PURPOSE:
4  GAINT PERFORMS GAUSSIAN INTEGRATION OF A
5  CONVOLUTION-TYPE INTEGRAL.
6  THE INTEGRAL IS DIVIDED INTO FOUR REGIONS:
7  1. A TO R-4.
8  2. R-4 TO R.
9  3. R TO R+4.
10 4. R+4 TO B.
11
12 DESCRIPTION OF PARAMETERS:
13 R - VALUE OF THE INDEPENDENT VARIABLE.
14 A,B - LIMITS OF INTEGRATION FOR THE DEPENDENT VARIABLE.
15 SUM - INTEGRAL VALUE RETURNED TO CALLING PROGRAM.
16 G,W - GAUSS ORDINATES AND WEIGHTS.
17 NDPS - NUMBER OF GAUSS POINTS.
18 P,PN - TRANSFORMED GAUSS ORDINATES AND WEIGHTS TO
19 THE REGION OF INTEGRATION (A,B).
20
21 SUBROUTINES AND FUNCTIONS REQUIRED:
22 F(R,F(I))
23 EXTERNAL FUNCTION DEFINING THE INTEGRAND FORM.
24
25 COMMON/CS/G(4),W(4),NDPS
26 DIMENSION P(4),PN(4)
27
28
29
30 SUM1=0.
31 SUM2=0.
32 IF(R-4.13,9,13)
33 IF(R15,5,9)
34 WRITE(6,7)
35 FORMAT(1X,"ERROR: R=0")
36 CALL EXIT
37
38 RMIN=A
39 C1=2.*(R-RMIN)
40 C2=RMIN
41 DO 11 I=1,NDPS
42 P(I)=C1*(1.+G(I))/(3.+G(I))+C2
43 PN(I)=W(I)*2.*C1/(3.+G(I)**2)
44 SUM1=SUM1+F(R,P(I))*PN(I)
45 GO TO 19
46
47 RMIN=R-4.
48 C1=2.*(R-RMIN)
49 C2=RMIN
50 DO 15 I=1,NDPS
51 P(I)=C1*(1.+G(I))/(3.+G(I))+C2
52 PN(I)=W(I)*2.*C1/(3.+G(I)**2)
53 SUM1=SUM1+F(R,P(I))*PN(I)
54 C1=2.*(RMIN-A)
55 C2=A
56 DO 17 I=1,NDPS
57 P(I)=C1*(1.+G(I))/(3.+G(I))+C2
58 PN(I)=W(I)*2.*C1/(3.+G(I)**2)
59 SUM1=SUM1+F(R,P(I))*PN(I)
60 IF((R+4.-B)29,21,21)
61 IF(R-8)23,27,27
62 RMAX=B
63 C1=2.*(RMAX-R)
64 C2=R
65 DO 25 I=1,NDPS
66 P(I)=C1*(1.+G(I))/(3.+G(I))+C2
67 PN(I)=W(I)*2.*C1/(3.+G(I)**2)
68 SUM2=SUM2+F(R,P(I))*PN(I)
69 SUM=SUM1+SUM2
70 RETURN
71
72 RMAX=R+4.
73 C1=2.*(RMAX-R)
74 C2=R
75 DO 31 I=1,NDPS
76 P(I)=C1*(1.+G(I))/(3.+G(I))+C2
77 PN(I)=W(I)*2.*C1/(3.+G(I)**2)
78 SUM2=SUM2+F(R,P(I))*PN(I)
79 C1=2.*(B-RMAX)
80 C2=RMAX
81 DO 33 I=1,NDPS
82 P(I)=C1*(1.+G(I))/(3.+G(I))+C2
83 PN(I)=W(I)*2.*C1/(3.+G(I)**2)
84 SUM2=SUM2+F(R,P(I))*PN(I)
85 SUM=SUM1+SUM2
86 RETURN
87
88 END

```

```

1      FUNCTION CONV(R1,R2)
      .....
5      PURPOSE:
      CONV IS USED IN CONJUNCTION WITH GAINT.
      EVALUATES THE NUCLEAR DENSITY-POTENTIAL FOLDING
      INTEGRAND USED IN GAINT FOR THE YUKAWA POTENTIAL.
10     DESCRIPTION OF PARAMETERS:
      R1 - INDEPENDENT VARIABLE.
      R2 - DEPENDENT VARIABLE OF INTEGRATION.
      AO - NUCLEAR SKIN THICKNESS.
      CO - NUCLEAR HALF-DENSITY RADIUS.
      RO - DENSITY NORMALIZATION CONSTANT.
15     DENS - WOODS-SAXON NUCLEAR DENSITY SHAPE.
      BETA - YUKAWA POTENTIAL INVERSE RANGE.
      SHAPE - YUKAWA POTENTIAL SHAPE AFTER ANGULAR INTEGRATION.
20     COMMON/C2/AO,CO,RO
      COMMON/C3/BETA
      COMMON/C4/HBAR,C,HBARC,SIGMAH,REDSN,THOPI,FOURPI
      C
25     SHAPE=R2*(EXP(-BETA*ABS(R1-R2))-EXP(-BETA*(R1+R2)))
      DENS=1/(1+EXP((R2-CO)/AO))
      CONV=THOPI*RO*SHAPE*DENS/(R1*(BETA**2))
      RETURN
      END

1      SUBROUTINE SCATL(VARY,SL)
      .....
5      PURPOSE:
      SCATL CALCULATES THE SCATTERING LENGTHS CORRESPONDING
      TO THE POTENTIAL VARIABLES CONTAINED IN THE ARRAY VARY.
      THE METHOD IS BASED ON AN INFINITE PRODUCT EXPANSION
      OF THE SCATTERING LENGTH AS A FUNCTION OF THE POTENTIAL
      DEPTH AND RANGE. ONLY THE FIRST FOUR TERMS OF THE
      EXPANSION ARE RETAINED HERE.
10     THE CONSTANTS SO,SZS APPEARING IN THE EXPANSION ARE
      SPECIFICALLY DEFINED FOR THE YUKAWA POTENTIAL. OTHER
      POTENTIAL PARAMETERS ARE LISTED IN THE ORIGINAL PAPER BY
      A. DELOFF, NUCL.PHYS.,4303,412(1973).
15     DESCRIPTION OF PARAMETERS:
      SL - ARRAY CONTAINING THE CALCULATED SCATTERING
      VO - COMPLEX ARRAY OF SIGMA-NUCLEON POTENTIAL DEPTHS.
      SO - LENGTHS RETURNED TO CHISOZ.
20     SZS - ARRAY OF CONSTANTS USED IN EXPANSION.
      VARY - ARRAY OF POTENTIAL PARAMETERS.
      BETA - INVERSE POTENTIAL RANGE.
25     COMPLEX SO,A,VC(50),SINT(50)
      DIMENSION VARY(50),SL(50)
      COMMON/C4/HBAR,C,HBARC,SIGMAH,REDSN,THOPI,FOURPI
      COMMON/C7/S(4),ZS(4)
      COMMON/C11/NSCATL,NSL(50),ERRSL(50)
30     COMMON/C12/INCEST
      C
35     VO(1)=CHPLX(VARY(1),0,1)
      VO(2)=CHPLX(VARY(2),0,1)
      VO(3)=CHPLX(VARY(3),VARY(4))
      VJ(1)=CHPLX(VARY(5),VARY(6))
      BETA=VARY(7)
      NP=NSCATL/2
      IF(INCEST.EQ.111,3)
40     WRITE(5,13)
      DO 11 J=1,NP
      SO=RECHSN*VO(J)/BETA**2
      AT(1,1)=1
      DO 5 4,1,4
      SINT(J)=*(1.-(SO/ZS(L)))/(1.-(SO/S(L)))
45     A=SINT(J)
      5 CONTINUE
      SINT(J)=-SO*SINT(J)/BETA
      SL(2*J-1)=REAL(SINT(J))
      SL(2*J)=IMAG(SINT(J))
50     IF(INCEST.EQ.117,9)
      7 WRITE(6,15)REAL(VC(J)),AIMAG(VO(J)),REAL(SINT(J)),-IMAG(SINT(J))
      9 CONTINUE
      11 CONTINUE
      13 FORMAT(/23X,"VO",35X,"SL")
55     15 FORMAT(/2X,2F15.8,5X/2F15.8)
      RETURN
      END

```



```

1      FUNCTION FACTOR(A)
2      *****
3      PURPOSE:
4      FACTOR CALCULATES A-FACTORIAL FOR REAL VALUES OF A.
5      STIRLINGS APPROXIMATION IS USED FOR A>11.
6
7      DESCRIPTION OF PARAMETERS:
8      A - INPUT: MUST BE A POSITIVE WHOLE NUMBER.
9
10     IF(A=1.0)GO TO 13
11     IF(A=11.0)GO TO 11
12     NA=FIX(A)-1
13     PROCT=A
14     DO 7 J=1,NA
15     7 PROCT=PROCT*(A-FLOAT(J))
16     FACTOR=PROCT
17     RETURN
18
19     IF(A.LT.0.)GO TO 13
20     FACTOR=L.
21     RETURN
22
23     STIRLA=(A+.5)*ALOG(A)-A+.9189385332
24     FACTOR=EXP(STIRLA)
25     RETURN
26
27     WRITE(6,15)
28     FORMAT(1,X,"ERROR: NEGATIVE ARGUMENT IN FACTOR")
29     CALL EXIT
30     END

```

## REFERENCES

- (1) C. J. Batty et al. Phys. Lett. B74, 27 (1978).
- (2) H. Koch. Proc. Int. Conf. High Energy Phys. Nucl. Struct: 5<sup>th</sup>, 225 (1974).
- (3) G. Alexander et al. Phys. Rev. D6, 2405 (1972).
- (4) S. Gasiorowicz. Elementary Particle Physics, John Wiley and Sons (1966).
- (5) C. E. Wiegand, G. L. Godfrey. Phys. Rev. A9, 2282 (1974).
- (6) D. Wilkinson. Proc. Int. Conf. Nucl. Struct., 215 (1960)
- (7) R. Seki. Phys. Rev. C5, 1196 (1972).
- (8) S. Gasiorowicz. Quantum Physics, John Wiley and Sons (1974).
- (9) A. Deloff, J. Law. Phys. Rev. C10, 1688 (1974).
- (10) G. Backenstoss et al. Phys. Lett. B43, 431 (1973).
- (11) B. L. Roberts et al. Phys. Rev. Lett. 32, 1265 (1974).
- (12) D. Zieminska. Phys. Lett. B37, 403 (1971).
- (13) R. Seki. Phys. Rev. Lett. 32, 132 (1973).
- (14) A. Deloff, Nukleonika, 22, 875 (1977).
- (15) A. Deloff. Phys. Rev. C13, 730 (1976).
- (16) T.E.O. Ericson, F. Scheck, Nucl. Phys. B19, 450 (1970).
- (17) A. Deloff. Nucl. Phys. A303, 412 (1978).
- (18) J. H. Koch, M. Sternheim. Phys. Rev. Lett. 28, 1061 (1972).
- (19) R. H. Dalitz. Nuclear Interactions of the Hyperons, Oxford University Press (1965).

- (20) A. Valk, Quantum Mechanics: Principles and Applications, Addison-Wesley (1973).
- (21) R. Newton, Scattering Theory of Waves and Particles, McGraw-Hill (1966).
- (22) F. Eisele et al. Phys. Lett. B37, 204 (1971).
- (23) Y. Gell et al. Nucl. Phys. B22, 583 (1970).
- (24) G. Fast, G. Ranft, J.J. De Swart, Nuovo Cimento, 34, 1242 (1964).
- (25) I.E. McCarthy, Introduction to Nuclear Theory, John Wiley and Sons (1968).
- (26) J.J. De Swart et al., Hyperon-Nucleon Interaction, University of Nijmegen, The Netherlands (1970).
- (27) H. Überall, Electron Scattering from Complex Nuclei, A, Academic Press (1971).
- (28) Landolt-Börnstein, Numerical Data and Functional Relationships, 2, Springer-Verlag (1967).
- (29) R. K. Bhaduri, Y. Nogami, W. Van Dijk, Nucl. Phys. B1, 269 (1967).
- (30) R. G. Dosch et al., Phys. Lett. 14, 162 (1965).